
ROYAL INSTITUTE
OF TECHNOLOGY

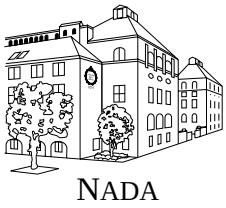

NADA
Department of Numerical
Analysis and Computer Science

# Synchrony, Excitability and Firing Frequency in Neurons Containing Dendritic A-type Potassium Currents

## Synkronicitet, excitabilitet och spikfrekvens hos neuroner som innehåller dendritiska kaliumströmmar av typ A

**Master's Thesis in Biomedical Engineering**

Vicente Charcos Lloréns
charcos@kth.se
*September 2003*

Supervisor: Erik Fransén
Examiner: Anders Lansner

*This page intentionally left blank*

# Abstract

**Synchrony, Excitability and Firing Frequency in Neurons Containing Dendritic A-type Potassium Currents**

Current interpretations of mental processes in neuroscience usually focus on the properties of either single nerve cells or of large networks of neurons. The interplay between the cellular and the network levels remains, however, poorly understood. Based on existing experimental evidence, we suggest a participation of A-type potassium channels ($K_A$) in the interaction between the two levels. In this project we investigate, more precisely, the role of $K_A$ in linking network synchrony to cellular excitability and firing frequency. The analysis of the notion of synchrony is of particular importance in this work due to its conceptual and modeling implications. The study uses computer simulations with biophysical models of cellular structures and of six different $K_A$ ion-channels described by Hodgkin-Huxley dynamics.

First, simple simulations reveal how $K_A$ can affect excitability and how the effects can be modified through $K_A$ modulation. The results indicate that the attenuating properties of $K_A$ should be interpreted in terms of absolute local attenuation. We show that other possible appealing interpretations are actually based on misconceptions. Additional results confirm a crucial role of $K_A$ in avoiding hyperexcitability, as suggested in several studies related to epilepsy. Thereafter, with more detailed models, simulations at different levels of synchrony prove that $K_A$, via its modulation, mediates between the network synchrony and the cellular response. This trilateral relationship suggests that mental activity resulting from the interaction between cells and networks could be altered through $K_A$ modulation. Finally, we discuss the possibility of preventing synchronization by means of dendritic ion-currents and propose, for this particular purpose, some favorable conditions regarding Hodgkin-Huxley variables.



***Key words:*** *Synchrony, excitability, firing frequency, A-current, $K_A$ channels, modulation, ion-channels, Hodgkin-Huxley dynamics, passive properties, neuron, network, synapse, EPSP, epilepsy, hyperexcitability, correlations, Poisson processes, gamma processes, computational neuroscience, GENESIS, NEURON, compartmental modeling, desynchronization.*

# Sammanfattning

**Synkronicitet, excitabilitet och spikfrekvens hos neuroner som innehåller dendritiska kaliumströmmar av typ A**

Nuvarande tolkningar inom neurovetenskapen av mentala processer fokuserar vanligen på egenskaperna hos antingen enskilda nervceller eller nätverk av neuroner. Förståelsen av samspelet mellan cell- och nätverksnivåer är emellertid liten. Grundat på redan existerande experimentella data föreslår vi att dendritiska kaliumkanaler av typ A ($K_A$) medverkar i samspelet mellan de två nivåerna. I detta projekt undersöker vi $K_A$:s roll för att binda synkronicitet i nätverk till cellulär excitabilitet och spikfrekvens. Analysen av begreppet synkronicitet är av särskild betydelse i detta arbete på grund av dess modellerings- och konceptuella konsekvenser. Arbetet är baserat på datorsimuleringar med biofysiska modeller av cellulära strukturer och sex olika $K_A$-kanaler med Hodgkin-Huxleydynamik.

Först visar enkla simuleringar hur $K_A$ kan påverka excitabilitet och hur efekterna kan modifieras genom modulering av $K_A$. Resultaten antyder att de dämpande egenskaperna hos $K_A$ bör tolkas i termer av absolut lokal attenuering och avslöjar även troliga missuppfattningar i förståelsen av dessa egenskaper. Ytterligare resultat stödjer en nyckelroll för $K_A$ när det gäller att undvika hyperexcitabilitet, såsom föreslagits i ett flertal olika arbeten relaterade till epilepsi. Därutöver visar simuleringar med mer detaljerade modeller av de två extremfallen av synkronicitet att $K_A$, genom dess modulering, är en länk mellan nätverkssynkronicitet och det enskilda cellsvaret. Detta ömsesidiga beroende antyder att den mentala aktiviteten orsakad av sambandet mellan celler och nätverk skulle kunna påverkas genom $K_A$-modulering. Slutligen diskuterar vi möjligheten att förhindra synkronisering med dendritiska jonströmmar samt föreslår några gynnsamma förutsättningar angående Hodgkin-Huxleyvariabler för detta ändamål.

***Sökord:*** *Synkronicitet, excitabilitet, spikfrekvens, A-ström, $K_A$-kanaler, modulering, jonkanaler, Hodgkin-Huxleydynamik, passiva egenskaper, neuron, nätverk, synaps, EPSP, epilepsi, hyperexcitabilitet, korrelationer, poissonprocesser, gammaprocesser, beräkningsneurovetenskap, GENESIS, NEURON, kompartmentmodeller, desynkronisering.*

# Foreword

This Master's Thesis is the final stage of my undergraduate engineering studies. It has been carried out within the context of my specialization in Biomedical Engineering and focuses on the area of Computational Neuroscience. As the work has progressed, my enthusiasm for the field of Biomedical Engineering has been nurtured and a deep interest in Neuroscience has aroused.

I would like to sincerely thank the following persons who have contributed in one way or another to the completion of this project:

- My supervisor Erik Fransén, for his high availability, his guidance and very fruitful and stimulating discussions at all levels. His expertise and human qualities have made of this project a challenging, rich and pleasant experience.
- Anders Lansner, for support and advice when I had to make important choices.
- Colleagues at *SANS*, the section for Studies of Artificial Neural Systems at the Royal Institute of Technology, and in particular my roommate Fredrik Edin, for providing a nice environment to work in.
- All the scientists who showed a positive attitude towards the interchange of ideas and thereby provided interesting and wise insights into specific problems.
- Finally, all the persons —friends and relatives— who have been patient, encouraging and supportive during this period of intensive work. In that respect, I am especially grateful to Amélie Darracq.

*This page intentionally left blank*

# Contents

# 1 Introduction

## 1.1 Background and problem definition

Understanding the interplay between the properties of individual nerve cells and those of the networks they are organized into is a major challenge in neuroscience. Indeed, by means of this interplay, the billions of neurons of the brain support processes ranging from "simple" motor actions to sophisticated cognitive tasks.

Historically, most studies in neuroscience have interpreted mental processes in terms of single nerve cells. A strong emphasis has been put on characterizing mental activity by the frequency with which neurons fire, *i. e.* they emit electrical pulses. Great interest has also been placed on excitability, which refers to the predisposition of nerve cells to fire, and on the factors that affect it.

A relatively recent perspective of increasing acceptance bases the interpretation of mental processes on network properties rather than on individual cells. This network perspective is supported by observations in *e. g.* EEG and fMRI[1] that associate a particular mental activity to specific areas of the brain. Other experimental results indicate synchronous cell firing activity within networks of several brain regions. Therefore, one class of theories links certain mental processes to the degree of synchrony in the firing of interconnected cells.

However, although synchrony is a network property, it is likely to interact with molecular mechanisms and cellular characteristics such as excitability or firing frequency. Epileptic seizures, for example, are usually described as the occurrence of large synchronizations associated to an enhanced neural excitability. Consequently, the first motivation behind this work is to identify and examine an electrophysiologically plausible link that relates synchrony, excitability and firing frequency, consistently with findings in current research.

As discussed in section 2.4, the specific A-type potassium ion-channel (hereafter called $K_A$ channel or $K_A$), which is present in many neural membranes, seems to be an excellent candidate. Further support of this particular choice is provided by Castro et al. (2001), Johnston et al. (2000b) and Zona et al. (2002), who suggest a key-role of $K_A$ in controlling excitability and epileptogenesis.

Therefore, as an attempt to bridge the gap between the cellular and the network levels, the purpose of this project is to analyze the particular relationships that arise between them in the specific case of the presence of $K_A$.

[1] Electroencephalograms and functional Magnetic Resonance Imaging respectively.

## 1.2 Project scope

Although a lot of effort has already been done in studying synchrony, as well as $K_A$ channels, many questions remain open, some of which are treated in this work. The most novel part of this study lies however in the analysis of the link that $K_A$ channels may represent between single cells (excitability, firing frequency) and the network they are part of (synchrony). The following objectives are set in order to tackle the defined problem:

- To review in the literature the known properties of $K_A$ channels and their associated functional roles (see section 2.5).
- To analyze the concept of synchrony and develop a satisfactory model of inputs of varying degrees of synchrony to a cell (sections 2.4 and 3.3).
- To examine how the presence of $K_A$ channels affects excitability, first in the simplified context of a passive piece of neural dendrite (section 4.1.1) and then with a spiking cell (see 4.1.2).
- To study how the mechanisms of excitability regulation by $K_A$ channels and the cell firing frequency differ at two extreme levels of synchrony in the network: highly synchronous (see 4.2) and totally asynchronous (see 4.3).
- To investigate the trilateral relationship between network synchrony, cell firing levels and cell excitability (see section 4.4).
- To explore favorable conditions for the existence of cellular desynchronizing mechanisms (section 4.5) that prevent the cell from participating in synchronous activity but not asynchronous.

These issues are addressed from a computational point of view, so no experiments have been done explicitly for this project. This first limitation is discussed in section 3.1.1. Another limitation has to do with the accuracy of the models, which is always a source of uncertainty in simulations, since small deviations from reality can result for example in important numerical divergences. Furthermore, a clear difficulty in this work is due to the complexity of the nervous system and to the relatively recent interest for $K_A$ channels. These factors result in a large size of the parameter space and in a relative shortage of data in each particular context.

Finally, it is important to mention that this project does not implement a network of cells, since there are no feedback connections. Instead, it studies phenomena at the cellular scale in an environment that mimics the input by the network. This approach aims at understanding and inferring the more complex relationships that would arise when going one step further and building the network.

# 2 Theoretical foundations

This chapter provides theoretical foundations for the understanding of the defined problem and the work carried out. It gives a general picture of neurophysiology and relevant useful statistical concepts. It also reviews the current knowledge on $K_A$ channels. Readers interested in further descriptions in neurophysiology can obtain them for example from Johnston and Wu (1999) or Kandel et al. (2000), in addition to the references suggested along the text.

## 2.1 Overview of the nervous system

Neurons are the elementary signaling units of the human nervous system, in which there are about one hundred billion. Neurons are very heterogeneous morphologically and functionally, with for example very divergent sizes, shapes or chemical contents. However, neurons have generally the same structure (see Figure 2.1): 1) a *cell body* known as *soma*, 2) a branched part called the *dendritic tree* with many *dendrites* (said *proximal* or *distal* depending on their distance to the soma) and 3) the *axon*, which corresponds to a cable-like structure that normally ends on a dendrite of another cell, in a structure of contact named *synapse*. By means of numerous synaptic connections, neurons form complex networks of communication.

Communication within networks corresponds to the propagation along a cell of *electrical potentials*, which are chemically transferred through synapses from the pre-synaptic axon to post-synaptic dendrites. The temporal and spatial summation of *post-synaptic potentials* (PSPs) along the dendrites is called *integration*. When the overall signal at the soma exceeds a certain *potential threshold*, a nerve impulse, named *spike* or *action potential* (AP), is sent along the axon and the cell is said to *fire*. The *firing frequency* has traditionally been considered the communication code that conveys the information in the nervous system, though other properties (*e. g.* the degree of synchrony among neurons) are currently proposed as alternative coding mechanisms.

Synapses are either *excitatory* or *inhibitory*, depending on whether the resulting post-synaptic potentials (*EPSPs* or *IPSPs* respectively) increase or decrease the probability of the post-synaptic neuron firing an action potential. In both cases, the synapse's effectiveness can be modified by many factors. A widely accepted principle introduced by Hebb (1949) suggests that the *synaptic strength* or *efficacy* is enhanced by previous use of the synapse.

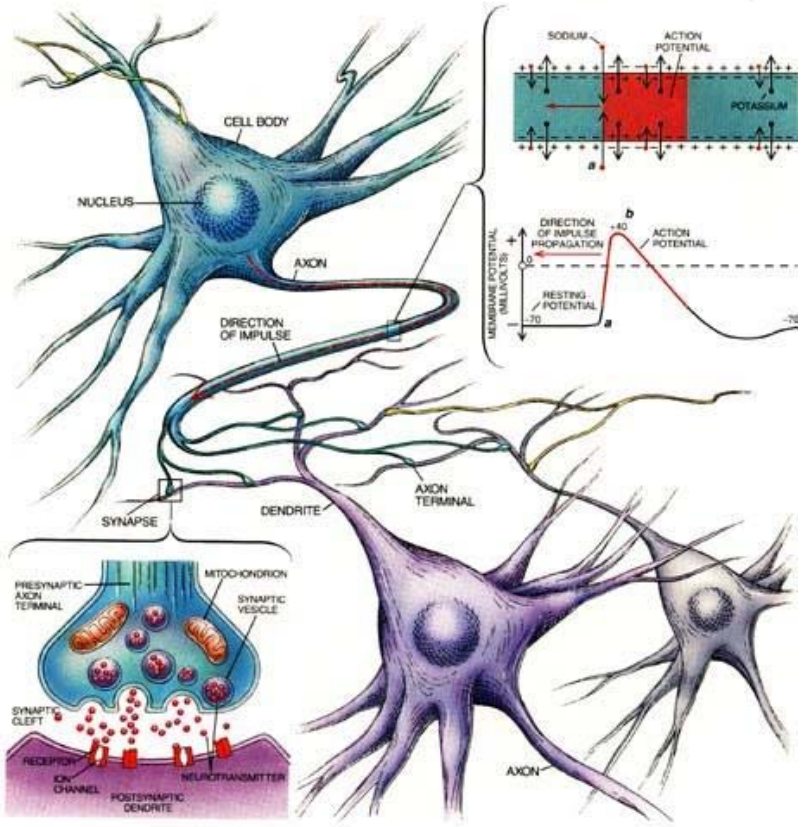


**Figure 2.1:** *Structure of a neuron.*
*Source: www.math.montana.edu/~pernarow/Stimulus_Response.html*

## 2.2 Ion-currents and channels

At rest, the distribution of ion species (mainly potassium $K^+$, sodium $Na^+$, chloride $Cl^-$ and calcium $Ca^{2+}$) in the neurons and the extracellular space maintains a potential difference across the membrane of about -70mV (interior more negative). As several physical mechanisms (*e. g.* diffusion or active transport) produce a flow of charges from and to the cell, transmembrane ion-currents appear, altering the transmembrane-voltage. The currents are said *depolarizing* or *hyperpolarizing*, depending on whether the resulting change in voltage is positive (*depolarization*) or negative (*hyperpolarization*). In fact, the electrical signals conveyed by neurons correspond basically to the propagation of membrane-voltage variations as ions flow across the membrane (see Figure 2.1).

The physical support for this movement of ions is provided by special membrane proteins called *ion-channels*. Since ion-channels are at the core of neural signaling, their malfunctioning can cause serious diseases. Moreover, they often constitute "the site of action of drugs, poisons, or toxins" (Kandel et al., 2000).

Ion-channels differ from one another essentially depending on the ion(s) they are permeable to and on the stimuli that causes them to open or close (*i. e.* their *gate*). Non-gated, voltage-, ligand- and mechanically-gated represent different common classes of channels. Important differences also exist in their location and density, with variations both along a single neuron and depending on type

of neuron and brain region. $Na^+$ and $K^+$ channels, for example, are present at the soma and axon, where they are responsible for the action potential (AP) generation and propagation, but they also exist in different proportions in dendrites. Neural structures containing only non-gated (leak) channels are said *passive*, whereas those with, for example, voltage-gated channels are known as *active*. The single unit conductance, which measures the ability of an individual ion-channel to conduct an ion, is also variable. All these and other distinctions result in a large range of channel families even within a given ion species.

## 2.3 Hodgkin-Huxley dynamics

Driven by the appropriate stimulus, ion-channels undergo conformational shifts between different states. Hodgkin and Huxley (1952) studied the effects of this process, called *gating*, on membrane conductance and ion-currents. They considered transitions between discrete states (*e. g.* open and closed). The probability $y(t) \in [0;1]$ of being in a certain state at time $t$ was described by means of a *gating variable* or *gate* $y$, for which they assumed first-order kinetics with rates $\alpha$ and $\beta$:

$$\underset{y(t)}{(open)} \overset{\beta(V)}{\underset{\alpha(V)}{\rightleftharpoons}} \underset{1-y(t)}{(closed)} \qquad \text{with} \quad \frac{dy}{dt} = \alpha(1-y) - \beta y, \qquad y(0) = y_0$$

$$\Longrightarrow y(t) = y_\infty + \left[(y_0 - y_\infty)e^{-t/\tau_y}\right], \qquad \underset{\text{(steady-state value)}}{y_\infty = \frac{\alpha}{\alpha+\beta}} \quad , \qquad \underset{\text{(time-constant)}}{\tau_y = \frac{1}{\alpha+\beta}}$$

Based on these hypotheses, Hodgkin and Huxley derived empirical equations describing the experimentally observed variations in membrane $Na^+$ and $K^+$ conductances (as functions of time and membrane-potential), denoted $g_{Na}$ and $g_K$. However, experimental conductance changes do not look as single exponentials but as power functions of them, so combinations of gates were used. More precisely, they found that $g_K(V,t) = n^4\bar{g}_K$ and $g_{Na}(V,t) = m^3h\bar{g}_{Na}$ where $\bar{g}_K$ and $\bar{g}_{Na}$ are the *maximum conductances* and $n$, $m$ and $h$ are gating variables. These gates depend on time as well as on $\alpha_y(V)$ and $\beta_y(V)$ ($y \equiv n, m, h$). Therefore, the current associated to, for example, $Na^+$ is:

$$I_{Na} = g_{Na}(V,t) \times (V - E_{Na}) = m^3(V,t) \times h(V,t) \times \bar{g}_{Na} \times (V - E_{Na})$$

where $E_{Na}$ is the equilibrium potential, which determines whether an ion-current is depolarizing or hyperpolarizing. Usually, $m$ and $n$ are called the *activation* variables because the corresponding gates open ($n$ and $m$ increase) when the cell gets depolarized. Conversely, $h$ is known as the *inactivation* variable because its gate closes subsequently ($h$ decreases, but more slowly), thereby inactivating the channel. Figure 2.2 shows the curves of the time-constants and the steady-state activation ($m_\infty$), inactivation ($h_\infty$) and *normalized conductance* ($\mathbf{g}_\infty = g_{Na}(\infty)/\bar{g}_{Na} = m_\infty^3 h_\infty$) found by Hodgkin and Huxley for $Na^+$.

This representation of changes in membrane ion-conductance has been widely used for many other voltage-gated channels. The principle has even been extended to other types of gates. According to Kandel et al. (2000), "a half century later, the Hodgkin-Huxley model stands as the most successful quantitative computational model in neural science if not in all of biology."

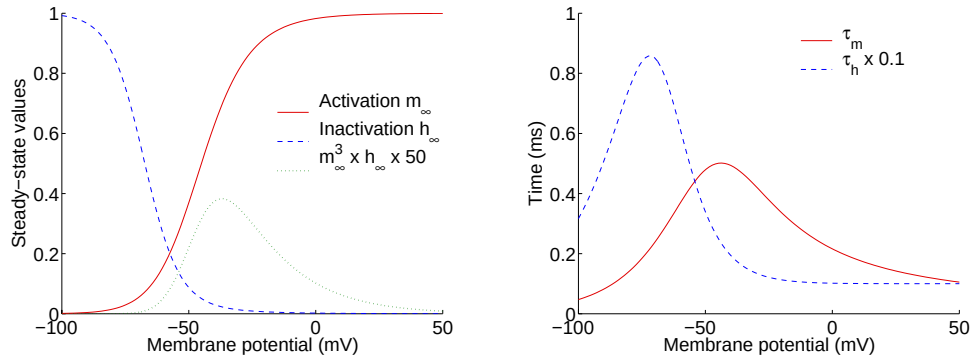


(a) (b)

**Figure 2.2:** *Voltage-dependence of (a) the steady-state activation, inactivation and normalized conductance and (b) their respective time-constants for the sodium channel (membrane resting-potential is -70 mV).*

## 2.4 Synchrony

### 2.4.1 Definition of synchrony

The concept of synchrony is related to network behavior. Briefly said, synchrony corresponds to the level of coincident activity of neurons in a network. In other words, if all neurons fire together, the network is said to be synchronized. Deeper considerations that take into account the statistical properties of neural firing (see section 2.6) introduce correlations among neural trains of spikes as a measure of synchrony. However, the presence of correlations does not always reflect synchronization, since different phenomena can produce similar correlations (Brody, 1999). Moreover, it seems reasonable to assume that asynchronous activity within groups of cells is generally somehow correlated, because the synapses between the cells compromise the independence of firing.

Another issue is whether synchrony should be defined pre- or post-synaptically. The above mentioned spike-timing coincidence is a pre-synaptic concept, because it does not depend on how the network activity continues to propagate through synaptic connections. Conversely, a post-synaptic definition could be based on EPSP coincidence, *i. e.* on the timing between post-synaptic signals measured *e. g.* at the soma. At the cellular level, the difference between spike and EPSP coincidence results from the dendritic location and propagation velocities of inputs to a cell. Indeed, simultaneous pre-synaptic signals might arrive asynchronously to the soma. Consequently, given a post-synaptic definition, synchronous activity favors EPSP summation, consistently with the commonly accepted idea of synchronization being efficient in producing spikes. The application of this post-synaptic definition to our work is discussed in section 3.3.

### 2.4.2 Importance of synchrony for mental processes

Synchronous neural activity has been experimentally observed and discussed in a multitude of functional contexts (Baker et al., 1999; Singer, 1999; Llinás et al., 2002). As previously mentioned, synchrony could even represent a coding

mechanism for neural signaling. Therefore, there might exist a close relationship between synchrony modulation and processing in the brain. Engel et al. (2001) suggest that "neural synchrony is crucial for object representation, response selection, attention and sensorimotor integration." Asynchronous activity, on the other hand, is seemingly involved in other functions such as working memory tasks (see *e. g.* Compte et al., 2003). Furthermore, failures in synchrony regulation have pathological consequences: enhanced synchronization, for instance, is characteristic of epilepsy and is associated in such cases to increased cell excitability.

### 2.4.3 Relationship between synchrony and cell properties

Several mechanisms are potentially capable of imposing a relationship between synchrony and cell behavior. This study aims at investigating one of these mechanisms compatible with the following requirements of biological relevance:

- Dependence on the degree of synchrony seen post-synaptically, to account for the observed increase in excitability usually promoted by synchrony;
- Energy efficiency, so that to avoid metabolic loads;
- Non-linearity, so that to react to high synchrony and hyperexcitability more than to other states, favoring the regulation presumed in normal tissue as opposed to epileptic conditions;
- Direct interaction between cell properties and the current degree of synchrony, rather than with previous states of synchrony, *i. e.* the effects of changes in synchrony must be immediate and not deferred.

Therefore, interesting candidates are post-synaptic, not energy-consuming, non-linear and intrinsic to the cell. These constraints exclude certain common intermediaries between synchrony and cell properties such as modulation via fluctuations in synaptic efficacies or activation of inhibitory interneurons. Active and energetically inefficient mechanisms are also discarded (ion pumps, leak currents, *etc.*). Conversely, dendritic voltage-gated channels seem well suited.

### 2.4.4 Crucial role of $K_A$ in synchrony

Several studies show evidence of the participation of $K_A$ channels in regulating excitability and epileptic synchronization. In particular, Castro et al. (2001) show that heterotopic pyramidal neurons in hippocampus, which are prone to epileptic hyperexcitability, fail to express the A-current. Moreover, they indicate that synaptic changes cannot explain their experimental observations and that "a hyperexcitability linked to excitatory/inhibitory neuro-transmission imbalance has not been reported." Furthermore, some compounds such as acetylcholine, which is known to influence $K_A$ and the cell integrative properties, also affect synchronization (Singer, 2003). Hess and El Manira (2001) also mention a role of $K_A$ channels "in regulating the excitability of neurons and the pattern of activity in a neural network." Hence, $K_A$ channels represent a plausible and particularly interesting mechanism relating synchrony to cell properties.

## 2.5 $K_A$ channels

The aspects of $K_A$ channels described in this section range from general concepts to specific details. The latter are essentially intended for those who are familiar with cellular neurophysiology and channel dynamics.

$K_A$ channels, as other potassium channels, are hyperpolarizing. They are gated by changes in voltage, producing the so-called A-current, also referred to as $K_A$-current, $I_A$-current, or transient current.

### 2.5.1 Location and distribution

$K_A$-currents are prominent in somatic and dendritic membranes of many mammalian neurons (Castro et al., 2001). They have been identified in several brain regions, among others in cortical cells (Johnston and Wu, 1999) like neocortical pyramidal neurons, hippocampal interneurons and hippocampal pyramidal neurons in regions CA1 and CA3 (Hoffman et al., 1997; Castro et al., 2001).

The density of $K_A$ channels also varies along the dendritic tree. In CA1 pyramidal neurons, the density increases linearly five-fold from the soma to about 350$\mu$m in the distal dendrites (Hoffman et al., 1997; Johnston et al., 2000b). Interestingly enough, these observations suggest a larger impact of $K_A$ on distal dendrites of CA1 pyramidal neurons.

### 2.5.2 Diversity

Although all observed A-currents share the same main properties, some divergences exist depending on the context: animal species, location in the brain, type of neuron, *etc.* These factors influence the channel dynamics, *i. e.* its activation ($m$) and inactivation ($h$) properties (time- and voltage-dependence).

An important distinction among $K_A$ channels is the voltage-range of activation, resulting in two major classes: low- and high-voltage activated $K_A$ channels (see Figure 2.3). Variations in voltage-ranges of activation can even be observed between channels proximal to the soma and those in the distal dendrites, the activation curve of the latter being shifted negatively.

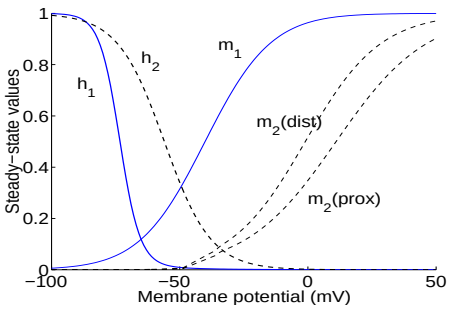


**Figure 2.3:** *Variations in voltage-ranges depending on $K_A$ type (1: low-activated or 2: high-activated) and dendritic location.*

The reason for these and other heterogeneities might lie in the multiplicity of genetic sources that have been associated to $K_A$ channels. For example, "only those belonging to the Kv3 gene family show a high voltage-range for activation" (Hess and El Manira, 2001). Even within this family, Kv3.4 inactivates about 25 times faster and is affected by different modulators than Kv3.3. Kv4.2 has also been linked to a specific part or subunit of a $K_A$ channel (Castro et al.,

2001). Coetzee et al. (1999) provide an overview of the genes coding for $K^+$ (including $K_A$) channel subunits and their genealogical relationships.

Consequently, the A-type current seems to correspond to a family of channels, whose classification requires further genetic, molecular, electrophysiological and pharmacological research.

### 2.5.3 Properties and functional role

Many studies of $K_A$ properties have been carried out in CA1 pyramidal cells in contexts related to epilepsy and, more recently, to *back-propagating action potentials* (BPAPs), *i. e.* APs propagating from the soma into the dendrites instead of along the axon. Therefore, many ideas developed in this section are derived from such studies but might apply to other contexts as well.

One of the most characteristic features of all $K_A$ channels is their rapid activation and their slower but still fast inactivation (Johnston and Wu, 1999; Johnston et al., 2000a; Castro et al., 2001; Hess and El Manira, 2001). Typical time-constants are about 0.1–10ms and 5–50ms respectively, although important deviations may exist owing to the mentioned diversity of $K_A$ channels.

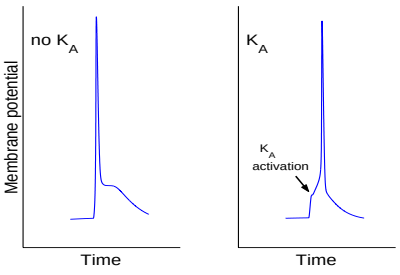


**Figure 2.4:** *Delay effect of $K_A$ .*

The rapid activation of the hyperpolarizing A-current makes it suitable for counteracting the onset of rapid depolarizations. Together with its subsequent rapid inactivation, this current has the transient (hence its name) effect of delaying (Figure 2.4), limiting or preventing the response to fast depolarizations (Hoffman et al., 1997).

Because of that, $K_A$ channels are thought to limit neural excitability (Johnston et al., 2000a; Castro et al., 2001; Zona et al., 2002) by 1) decreasing the amplitude of EPSPs, thereby raising the threshold for spike initiation (Hoffman et al., 1997) and 2) limiting the amplitude of BPAPs (Hoffman et al., 1997; Johnston et al., 2000b). As a result, A-currents are also able to control the neuron's AP firing frequency (Hess and El Manira, 2001), thereby contributing to *spike frequency adaptation* during long membrane depolarizations (Castro et al., 2001). $K_A$-currents could even affect the cell firing mode and lead to transitions from single regular spiking to bursting (Johnston et al., 2000b). It should be noted that the role of $K_A$ is most often discussed in connection with large depolarizations, but little is said about its impact on smaller depolarizations. This issue is tackled in chapter 4 when presenting the results of this work.

Additionally, $K_A$ channels are believed to participate in spike repolarization and to contribute to the resting-potential. The latter effect is obtained for $K_A$ channel-types that are active at rest, *i. e.* with a non-negligible steady-state normalized conductance at resting-potentials.

All these properties are likely to make the cell response sensitive to changes in the density or dynamics of $K_A$ channels. Therefore, it must be emphasized that regulation of this channel represents a key-issue in the context of this project.

### 2.5.4 Pharmacology and Modulation

$K_A$ channels are blocked by 4-aminopyridine (4-AP) at concentrations higher than 100$\mu$M in a dose-dependent manner (Hoffman et al., 1997; Johnston and Wu, 1999; Johnston et al., 2000a; Castro et al., 2001; Zona et al., 2002). However, Hess and El Manira (2001) point out that 4-AP blockade is poorly reversible and not specific: the sustained current $K_D$ is more strongly affected. Instead, they propose catecholamine as a selective and reversible $K_A$ blocker. This blockade is dose-dependent but voltage-independent, *i. e.* similar at different potentials. Hoffman et al. (1997) also report a partial blockade of $K_A$ by dendrotoxin (DTX). On the contrary, lamotrigine (LTG), which is an anticonvulsant drug used for epilepsy, enhances neocortical potassium currents identified by Zona et al. (2002) as A-currents, also in a dose-dependent way.

Concerning changes in $K_A$ dynamics, the presence of GABA ($\gamma$-aminobutyric acid) or baclofen leads, in mammalian hippocampal neurons, to a positive voltage-shift of $K_A$ activation and inactivation (Saint et al., 1990). Conversely, negative shifts occur via muscarinic modulation (Akins et al., 1990), *i. e.* under the influence of muscarinic agonists such as acetylcholine (ACh). Note that "activation of muscarinic receptors is functionally significant, particularly in Parkinson's disease" (Akins et al., 1990). Moreover, the activation of the neocortex required for the manifestation of precise response synchronization is mediated by acetylcholine via muscarinic receptors (Singer, 2003).

Shifts in voltage are also possible, both positively and negatively, by means of neurotransmitters and second messenger systems (Johnston et al., 2000b). Activation or inhibition of different protein kinases (PKA, PKC, MAPK), many of which are known to operate in region CA1 of the hippocampus (Johnston et al., 2000a), modify $K_A$ dynamics, for instance by affecting the activation of muscarinic receptors. Hoffman et al. (1997) suggest that $K_A$ activity "is controlled by neurotransmitters, chemical messengers, cation concentrations, auxiliary subunits, and by oxidative and phosphorylation states."

$K_A$ dynamics also change with temperature variations, as for most ion-channels. Indeed, a high $Q_{10}$[1] leads to faster kinetics with raises in temperature.

Finally, one of the major modes of $K_A$ regulation is provided by changes in local membrane-potential. Although this is an inherent property of any voltage-gated channel, it especially affects $K_A$ due to its rapid dynamics. Furthermore, due to the presence of both activation and inactivation, prior depolarizations to a cell by trains of EPSPs or subthreshold activity (*i. e.* not producing spikes) can inactivate $K_A$ channels and improve cell excitability (Hoffman et al., 1997; Johnston et al., 2000a,b). Note that the efficiency of this dynamic regulation is, in fact, one of the main sources of complexity in this and other studies of the mechanisms associated to $K_A$.

The large number of agents and mechanisms involved in the regulation of either the density or the dynamics of $K_A$ channels is presumably indicative of the importance of A-currents, as suggested by Hoffman et al. (1997).

[1] $Q_{10} = r_2/r_1$ where $r_1$ is the rate of reaction at a given temperature $T$ and $r_2$ is the rate for a 10°C increase in temperature ($T + 10$°C), see *e. g.* Johnston and Wu (1999, p. 377).

## 2.6 Statistics

As in other areas of biology, many neurophysiological processes are not deterministic but probabilistic. Therefore, neuroscientists require statistical tools as a basis for stochastic descriptions. This section introduces some of these tools. However, a basic background in probabilities and statistics is assumed. Readers unfamiliar with concepts like random variables or distributions are encouraged to consult one of the abundant textbooks or Internet resources on these topics.

### 2.6.1 Neural firing as a Poisson process

The spiking of neurons is often regarded as a Poisson process whose rate is the average firing frequency. This means that the time of occurrence and the actual number of spikes in any specific time-interval is unpredictable, even though the average number of events is known. This unpredictability is illustrated in Figure 2.5 for a neuron firing at an average rate $\lambda = f = 5Hz$:

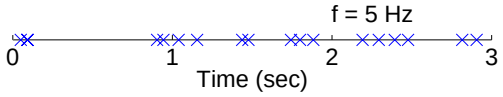


**Figure 2.5:** *Poisson process representing the random times of occurrence (marked by crosses) of spikes in a neuron firing at 5 Hz*

However, given a specific time-interval, the probability of firing $x \in \mathbb{N}$ action potentials is given by: $\mathcal{P}(x) = \frac{\mu^x e^{-\mu}}{x!}$, where $\mu$ is the average number of events for the length of the interval ($\mu = \lambda$ for a one-second interval). Figure 2.6 represents these probabilities for an interval of one second with two different rates. In both cases the maximum probability is of course located at the average value $\mu$ of the number of spikes.

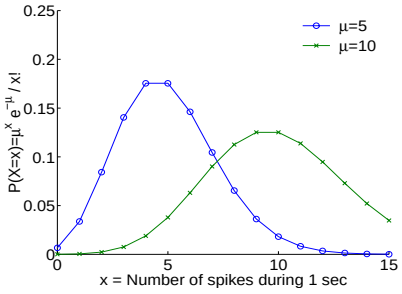


**Figure 2.6:** *Poisson probabilities.*

Moreover, the interspike interval in such a Poisson process is a random exponential variable of the same rate. Consequently, given a spike at time $t_1$, the probability of waiting a time $t \geq 0$ until next spike is: $\mathcal{P}(t) = \lambda e^{-\lambda t}$. The average time between successive spikes is then $1/\lambda$.

Conversely, given a stochastic process (*e. g.* a train of spikes), if the count of interspike intervals as a function of their duration matches an exponential density function, then it is a Poisson process. A Poisson process can hence be easily obtained by generating exponential random *variates*, *i. e.* by creating pseudo-random numbers with a distribution matching that of an exponential variable. It is thus possible to mathematically reproduce the firing pattern of a spiking neuron.

### 2.6.2 Gamma distributions

A random variable $X$ with a gamma distribution of shape parameter $k$ and rate $\lambda$ can be described, based on a Poisson process of same rate $\lambda$, as the waiting-time from a given spike until the $k_{th}$ next spike. The case $k = 1$ corresponds, according to the previous remarks, to an exponential distribution. The probability of this waiting-time being $t$ is:

$$\mathcal{P}(X = t) = \frac{\lambda^k t^{k-1} e^{-\lambda t}}{(k-1)!} \qquad \text{with} \quad t \geq 0, \quad k \in \mathbb{N}^*$$

The gamma distribution can be generalized to non-integer shape parameters $\alpha \equiv k$ and especially to the case $0 < \alpha \leq 1$:

$$\mathcal{P}(X = t) = \frac{\lambda^\alpha t^{\alpha-1} e^{-\lambda t}}{\Gamma(\alpha)} \qquad \text{with} \quad t \geq 0, \quad \alpha > 0$$

$$\text{and} \quad \Gamma(\alpha) = \int_0^\infty t^{\alpha-1} e^{-t} dt$$

An interesting property of the gamma distribution is that if $X_1$ and $X_2$ are independent gamma variables $\gamma_{X_1}(\alpha_1, \lambda)$ and $\gamma_{X_2}(\alpha_2, \lambda)$ , then $X_1 + X_2$ is $\gamma_{X1+X_2}(\alpha_1+\alpha_2, \lambda)$. Therefore, by sequentially generating random numbers from $n \geq 1$ independent gamma variables $X_1, \ldots, X_n$ with distributions $\gamma_{X_i}(\alpha_i, \lambda)$, $\gamma(1, \lambda)$ variables are obtained, *i. e.* exponential variables. Provided that these exponential variables describe interspike intervals, this procedure produces $n$ correlated Poisson processes as illustrated in Figure 2.7. This technique suggests a method for modeling the firing of correlated neurons[2] (see section 3.3.3).

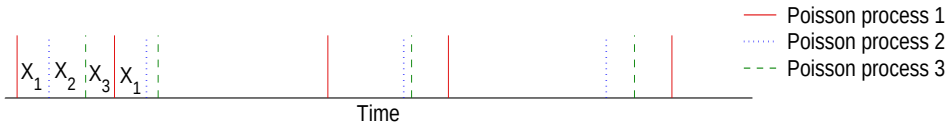


**Figure 2.7:** *Correlated Poisson processes of 3 spiking neurons. Intervals are generated sequentially from gamma random variables $X_1$, $X_2$ and $X_3$ with shape parameters summing to unity.*

[2]This idea was proposed by Bruce Knight and is described in Jonathan D. Victor's website at http://wwwusers.med.cornell.edu/~jdvicto/jdvunso.html

# 3 Methods

This chapter examines the methods and models that have been used in this project. It also states and justifies the different assumptions and choices that have been necessary. The first section presents general principles in neural modeling. Then, section 3.2 describes the models of ion-channels and cells that have been studied. Finally, section 3.3 explains how the input by the network to the cell has been simulated.

## 3.1 Modeling principles in neuroscience

### 3.1.1 Computational and experimental approaches

Computational simulations and experimental research currently represent two major approaches in neuroscience. Although they are sometimes seen as divergent, they are actually complementary. Whereas experimental studies provide for example highly valuable electrophysiological data, numerical simulations often result in cost- and time-efficient interesting predictions. However, numerical results should always be controlled experimentally because they normally involve a considerable amount of simplifications.

This study is computationally oriented, although the models are developed based on multiple experimental observations. In addition, results are checked for consistency with existing experimental findings in relevant areas.

### 3.1.2 Compartmental modeling

Numerical simulations of neurophysiological systems are frequently founded on a technique called *compartmental modeling*, which makes use of *cable theory*. The key-idea of this technique consists in finding electrical analogues of the neural structures, including dendrites, soma and axon. An accurate analogy depends upon the anatomy of each of these structures, which is usually approximated by geometrical forms like spheres (*e. g.* soma) and series of cylinders (*e. g.* axon, dendrites) of varying diameter and length. This approximation, known as the *cable model*, enables a computation of voltage propagation based on the continuous equations of cable theory.

The geometrical shapes can then be characterized by electrical parameters derived from the functional properties of the neural structures, such as the membrane resistivity ($R_m$), the membrane capacitance ($C_m$) and the intracellular

axial resistance ($R_i$). This process of abstraction leading to an equivalent representation of neurons by discretized electrical circuits is the essence of compartmental modeling (see Figure 3.1). It relies heavily on the solid mathematical and physical knowledge of core conductors, especially of *cable properties*. Moreover, the equivalent electrical description of neurons can in some cases be simplified by means of the Rall model. This model suggests a possibility of substituting complex branched dendritic trees by mathematically and electrically equivalent single cylinders, thereby reaching significant levels of *model reduction*. Finally, the electrical descriptions of other elements such as ion-channels and synapses are grafted onto the model at the appropriate compartments in order to complete the representation.

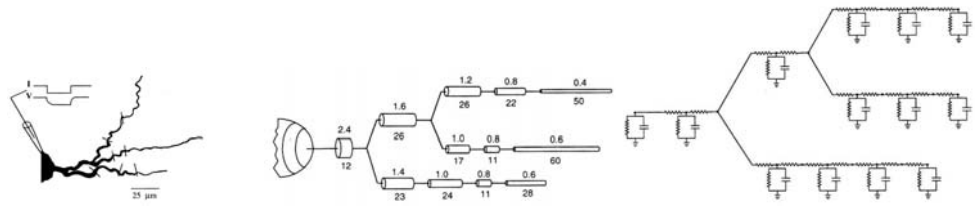

(a) Neuron (b) Cable model (c) Compartmental model

**Figure 3.1:** *Equivalent electrical representation of (a) a morphologically and physiologically characterized neuron: (b) geometrical approximation and (c) circuit analogy. Reproduced from Koch and Segev (1998). Courtesy of Idan Segev.*

The mathematical and electrophysiological details of these modeling procedures and the theory behind them are thoroughly explained by Koch and Segev (1998) and Johnston and Wu (1999). It is outside the current scope to describe the range of equations that determine a cell's or network's behavior. Several modeling software packages offer a convenient framework for compartmental modeling, in which these equations are already implemented. These programs also provide adapted tools for the numerical resolution of the involved differential equations. Two of them, namely GENESIS and NEURON[1], have been used in two different parts of this project as specified in sections 3.2.2 and 3.2.3 respectively.

### 3.1.3 Performance and computing issues

Several common computing principles aiming at improving the performance of the simulations have been applied in this work. Among others, the following measures have been taken: 1) run of simulations in console mode, *i. e.* without the substantial overload of graphical output; 2) storage of necessary values in memory rather than repeated calculations, sparing thus processing resources; 3) use of different clocks or integration-step sizes adapted to the time-scales of evolution of the various simulation elements; 4) use of efficient methods of numerical integration, guaranteeing both speed and accuracy.

The use of GENESIS and NEURON as modeling programs has been complemented by the use of the technical mathematical environment Matlab® for the efficient analysis of the results.

[1]See http://www.genesis-sim.org/ and http://www.neuron.yale.edu/neuron/ respectively.

## 3.2 Biophysical models

### 3.2.1 Models of $K_A$ channels

Several Hodgkin-Huxley descriptions of $K_A$ channels based on solid experimental results are available in the literature. We have identified a total of six different such descriptions of $K_A$ channels that we have investigated along this work. They originate from Connor and Stevens (1971), Huguenard and McCormick (1992), Hoffman et al. (1997), Traub et al. (1991), Yamada et al. (1998) and Migliore et al. (1999). Hereafter, the channels will be referred to as CS71, HMcC92, Hoff97, Traub91, Yama98 and Mig99 respectively.

The normalized conductances of the channels have the empirical form $\mathbf{g} = m^4h$ in the first three cases and $\mathbf{g} = mh$ in the other three. The expressions defining their dynamics and the associated plots are specified in Appendix A. Their differences, visible in Figure 3.2, reflect the diversity previously mentioned in section 2.5.2. A comparative study of how these divergences affect the cell's integrative properties in several contexts is carried out in section 4.1.1 by means of a simple model of a passive dendrite.

A model of each of the six mentioned channels normally exists already in one of the two databases associated to the used simulation packages. In this project, the six channels have been modeled with GENESIS for the comparative study on the passive dendrite. Models of all six have also been created with NEURON, although only Mig99 has been extensively investigated in this context.

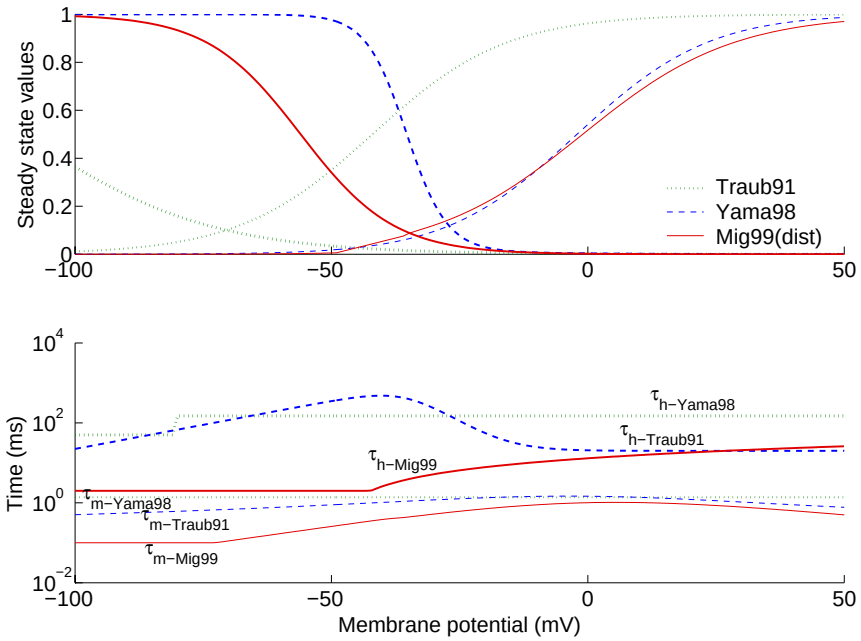


**Figure 3.2:** *Diversity of used $K_A$ channels: comparison of [Top] steady-state variables $h_\infty(V)$ (decreasing, thicker curves) and $m_\infty(V)$ (increasing, thinner curves), and [Bottom] time-constants, in log scale. Note the significant differences in voltage-ranges, slopes and time-constants. For the sake of clarity, only three channels (and only their distal component if relevant) representative of these differences are shown, among which Mig99 — the most used in this work.*

### 3.2.2 Simple model of passive dendrite

As part of a preliminary and necessary study, a simple compartmental model corresponding to a passive piece of dendrite has been developed. The simplicity of the model is expected to contribute to a better understanding of the described mechanisms by which $K_A$ regulates excitability, as well as to a better characterization of the six selected $K_A$ channels.

The model simulates a passive piece of dendrite, *i. e.* without voltage-dependent channels. It consists of 50 identical compartments of a length of 50 $\mu m$ and a diameter of 1 $\mu m$. The specific membrane resistivity is $R_m = 10k\Omega.cm^2$, the specific membrane capacitance $C_m = 1\mu F/cm^2$ and the specific intracellular (axial) resistivity $R_i = 0.1k\Omega.cm^2$. The resting-potential is $E_{rest} = -60mV$.

The model has been created with GENESIS (Bower and Beeman, 1994), the GEneral NEural SImulation System, and is an extended and customized version of a tutorial. The model is shown in Figure 3.3.

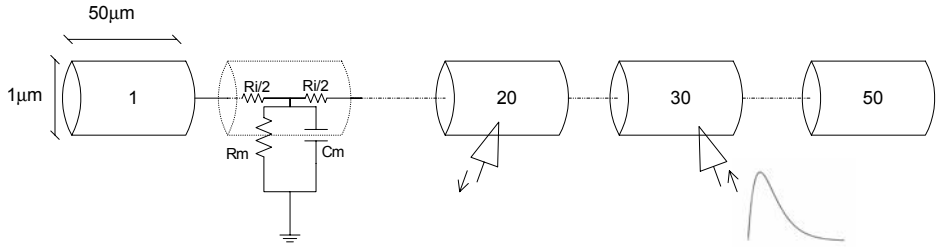


**Figure 3.3:** *Compartmental model of piece of dendrite, with 50 identical compartments. The equivalent passive circuit is only represented in one compartment. Inputs are delivered into compartment 30 and the potential is observed at compartment 20.*

The purpose is to analyze the effects of $K_A$ channels on the amplitude of propagating EPSPs in a variety of contexts: shifts in voltage-range of activation, changes in channel densities and temperature variations. Single EPSPs are generated via synaptic inputs. Synapses have a reversal potential of $E_{syn} = -10mV$. Their conductance changes are described as "alpha functions" with a time-constant $\tau_{syn} = 1ms$ (see Appendix B), corresponding to an AMPA synapse. The maximum conductance $g_{syn}$ is varied by steps of 0.4nS from 0 to 80 nS. These boundaries ensure reasonable changes in transmembrane potential at the site of input ($0 \leq \Delta V \leq +40mV$).

EPSPs are then recorded both at the site of input (the $30^{th}$ compartment) and at a distant compartment (number 20), both chosen somewhat arbitrarily. Simulations are run for 25–50 ms, first in control conditions, *i. e.* without $K_A$, and then with $K_A$ channels added to the dendrite, one at a time, with uniform densities. For each of the channels, the density has been set arbitrarily to a value within reasonable limits and causing measurable effects on the EPSP. The equilibrium potential of $K^+$ has been set to $E_K = -75mV$. A constant time-step of 0.01 ms is chosen. The Crank-Nicholson method for numerical integration has been used in conjunction with the `hsolve` object, which speeds up the simulation by, for example, allowing for larger integration time-steps (see Bower and Beeman, 1994, chap. 19).

### 3.2.3 Detailed spiking cell models

A deeper understanding of the interactions mediated by $K_A$ channels between synchrony levels and cell properties requires, however, a more complex and detailed framework than that of the simple model described above. The model should also take into account, among others, voltage-dependent ion-channels, multiple synapses and cell morphology. The inclusion of a firing threshold is indispensable for the analysis of spike production, which is a core component of this work.

Since many of the studies of $K_A$ have been performed in CA1 pyramidal cells (see 2.5.3), it seems appropriate to focus on this type of neuron. Indeed, experimental data is already available concerning *e. g.* the distribution of $K_A$ and other ion-channels along the cell. Besides, this choice will enable a comparison with existing experimental observations. Although detailed CA1 pyramidal cell models do not abound, NEURON's database provides one with many details. This model is the one used by Poolos et al. (2002), which actually originates from Migliore et al. (1999). It is based on relatively exhaustive descriptions of the geometry, electrophysiological parameters and ion-channels of a CA1 neuron experimentally studied by Pyapali et al. (1998) and shown in Figure 3.4. Since the model has been conceived with NEURON (see *e. g.* Hines and Carnevale, 1997), the use of this program to run the simulations seems a natural choice.

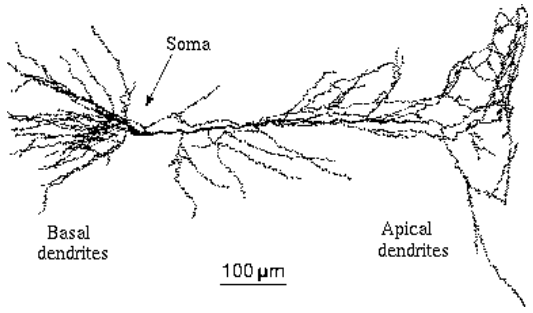


**Figure 3.4:** *Morphology of the modeled CA1 pyramidal nerve cell. Courtesy of Dennis Turner. Experimental data from Pyapali et al. (1998). Figure adapted from www.neuro.soton.ac.uk/~jchad/cellArchive/cellArchive.html*

The model includes 202 compartments: 13 somatic, 127 for apical dendrites, 60 for basal dendrites and two for the axon. Beyond its passive properties, it contains an assortment of ion-channels with Hodgkin-Huxley dynamics: $Na^+$, $K_{DR}$ (delay-rectifier), h-channel (hyperpolarization-activated) and $K_A$, with several variants depending mainly on their location on the cell. The resting-potential is taken at $E_{rest} = -65mV$ and the temperature is assumed to be $34°C$. Dual exponential functions are used for synaptic conductances (see Appendix B). Synapses have a reversal potential $E_{syn} = 0V$. Further details about the original model can be obtained from the two articles mentioned above.

Alterations made in this project to the model of Poolos et al. affect, among others, the voltage-shift in $Na$ dynamics (set to 5mV instead of 15mV) and the maximal conductances of $K_A$, which are increased. These two changes are actually based on the values originally proposed in the work of Migliore et al. (1999), which focused on $K_A$.

More crucial modifications of the model concern synapses. Synaptic inputs are not modeled as population inputs but as many individual, single synapses receiving trains of spikes at 12 Hz (see section 3.3). As a result, the time-constants have been set to $\tau_1 = 1.5ms$ (rise) and $\tau_2 = 2.5ms$ (decay) corresponding to excitatory AMPA synapses. Magee and Cook (2000) showed that, in CA1 pyramidal neurons, the somatic EPSP amplitude is independent of synapse location. Consequently, the model has been simplified by locating all synaptic connections on the same distal apical compartment, at about 210 $\mu$m from the soma. This decision is also related to the post-synaptic definition of synchrony as a time-window for EPSP summation (see 2.4.1). However, since the total number of inputs to the cell varies from 10 to 1000 in different simulations and the synaptic strengths are scaled accordingly, the somatic EPSP amplitude produced by a single input is not identical for all simulations.

The considerable number of synaptic connections, the complex cell morphology and the relatively long time-scales (simulations of up to 1500 ms) have required efficient tools for numerical integration. The model makes use of `CVode`, defined in the documentation as a multi-order variable time-step integration method which results in substantial performance benefits (factor of more than 10).

The model is first used to complement the previous study (passive dendrite) of the role of $K_A$ in excitability regulation with this more realistic situation, which incorporates active components and a spiking threshold. Then, the role of $K_A$ is examined with multiple inputs to the cell in the extreme cases of perfectly synchronous and totally asynchronous activity. Finally, the model is exploited to analyze the complex relationships that might arise between graded levels of synchrony and cell firing.

Note that the results obtained with graded levels of synchrony have been validated by means of another —more reduced— model of a cortical pyramidal cell. This simplified eight-compartment model was proposed by Bush and Sejnowski (1993). Together with ion-channels from Lytton and Sejnowski (1991), it has been implemented into NEURON and developed by Eriksson (2002) and later by Svennenfors (2003) in order to account for calcium buffers and dynamics. The model has been refined in this project by adapting it for the use of the efficient `CVode` and, of course, $K_A$ has also been added to the pool of ion-channels.

## 3.3 Models of network inputs to the neuron

As pointed out by Poirazi et al. (2003), "conclusions regarding synaptic arithmetic can be influenced by an array of seemingly innocuous experimental design choices." Therefore, it is important to describe and motivate the modeling solutions for synchrony and synaptic input that have been adopted. Note that the issues addressed hereafter represent modeling work carried out specifically within this project.

### 3.3.1 Synchrony as a time-window for EPSP summation

According to Brody (1999), experimentally measured correlations between neurons might correspond to other phenomena than synchronous activity. More-

over, for the post-synaptic cell to perceive inputs as synchronous, the resulting EPSPs must coincide at some point of the cell (*e. g.* the soma). This poses serious constraints on the timing between inputs in relation to the location of the synapses and the propagation velocities of EPSPs.

Consequently, the concept of synchrony has been defined in this project post-synaptically, as a time-window for EPSP summation. The time-window is the *average* duration over which the EPSPs are distributed. The more simultaneous (statistically) the EPSPs, the narrower the time-window and the higher the synchrony. The degree of synchrony $s$ (in %) is then determined by the ratio $r$ between the length of the time-window ($T_w$) and the average firing period of the network ($T_0$): $s = 100 \times (1 - r) = 100 \times (1 - T_w/T_0)$. A ratio $r$ close to 1 corresponds to EPSPs that are distributed over time. EPSP summation is then minimal, so the activity in the network is asynchronous. On the contrary, with significant EPSP summation, $r$ tends to 0, corresponding to high levels of synchrony. Other ratios determine intermediate degrees of synchrony. For instance, when inputs whose frequency is 10Hz (average period of 100ms) generate EPSPs that are distributed, on average, within time-windows of 30ms, the inputs have a synchrony of 70%.

However, due to the inherent randomness of spiking, the actual EPSPs are not exclusively restricted to the average time-window. In the example above, EPSPs from all inputs would theoretically arrive within 30ms every 100ms, although in practice both values are only average durations (see Figure 3.5).

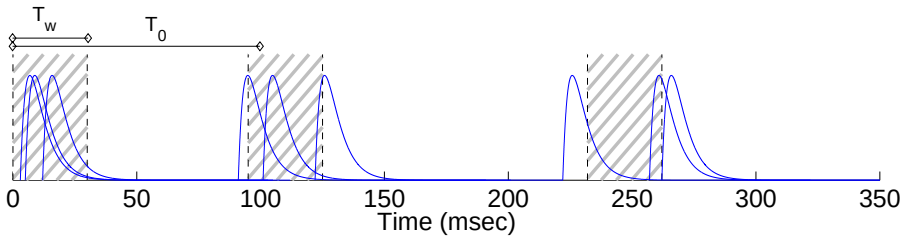


**Figure 3.5:** *Three inputs whose frequency is 10Hz synchronized at 70%. The time-window (dashed region) is then 30ms long, which is the average duration for the distribution of EPSPs. Note that both the occurrence of EPSPs at any time-window and the intervals between windows are random, reflecting the inherent unpredictability of neural firing. For clarity, EPSPs are superimposed and not summed.*

It is important to observe that, given this model, synchronization results in high but short depolarizations (strong coincidence within a narrow time-window), whereas desynchronization causes much lower but sustained depolarizations. Figuratively, with a sufficiently high number of inputs, synchronous activity corresponds to AC oscillations with a small duty-cycle and asynchronous activity to a DC signal.

Note that this model of synchrony only indicates average time-boundaries for EPSP summation, but it does not constrain the distribution of synaptic pulses within the time-window. As a result, a representation must be developed for the time-distribution of synaptic inputs at any level of synchrony. Different possible representations are discussed in the following section.

### 3.3.2 Time-distribution of inputs within the time-window

As mentioned in section 3.2.3, page 18, because of the independence of somatic depolarization from synaptic dendritic location, all synaptic connections have been established at the same compartment. This decision greatly simplifies the representation of the distribution of inputs during the time-window.

One straightforward modeling solution consists in merging all the inputs into one unique population EPSP occurring within the time-window. The amplitude of the population EPSP can be adjusted to account for different population sizes. By adjusting then the time-constants of the population EPSP, the input can be restricted to the desired time-window, *i. e.* the desired level of synchrony. Despite the simplicity of this solution, the representation of multiple synaptic events by a smooth population EPSP fails to express the high-frequency potential variations that actually occur within the time-window (see Figure 3.6). These rapid variations —which result from the relationship between the number of inputs, their average frequency and the exact time-course of single EPSPs— might affect the firing of the cell and its mechanisms of excitability, especially rapid mechanisms such as $K_A$ channels. For example, in the case of Figure 3.6, the rapid variations might make some of the summed EPSPs result in spikes and other not, whereas the four population EPSPs would most probably lead to the same response.

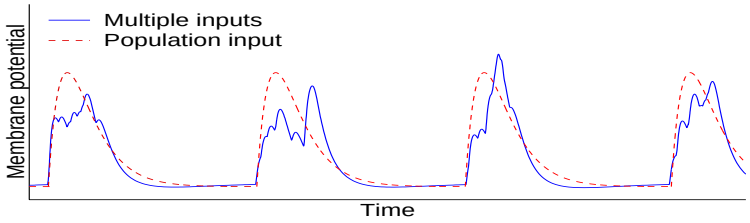


**Figure 3.6:** *Potential variations obtained with multiple (solid line) and population (dashed) inputs. The latter lead to smooth EPSPs that fail to express potential variations of higher frequency.*

As a result, the use of multiple synapses associated to the different presynaptic cells seems to be a better modeling alternative than population EPSPs. In line with this idea, Poirazi et al. (2003) also indicate the necessity of extending their studies of synaptic integration to more realistic situations with, among others, multiple synaptic inputs. However, a high number of synapses leads to substantial computational loads, so the number of synaptic inputs has been limited to 1000, which is a biologically reasonable amount of concurrent inputs.

The distribution of these multiple inputs can be modeled by means of several probability functions, such as square, triangular or gaussian functions. The choice among the three represents an interpretation of synchrony at the detail level. Any decision is therefore somewhat arbitrary and debatable, although the three modeling solutions seem pertinent. From a computational point of view, a square function has been preferred in this project for simplicity reasons. The consequence is that synaptic events are statistically equally distributed over the whole time-window. To sum up, the multiple synaptic inputs to the neuron are described by:

- Their degree of synchrony, represented by an average time-window dividing the whole time-scale into (statistically) active and inactive intervals;
- Their time-distribution within the active interval, represented by means of a square probability function (uniform distribution).

The actual generation of events satisfying these criteria (given degree of synchrony and uniform distribution) is discussed in the following section.

### 3.3.3 Numerical implementation

A conceptually appealing solution to generate equally distributed events over the time-window is inspired by the observations made in section 2.6.2 concerning gamma distributions. The idea consists in using gamma variables and a set of artificial presynaptic neurons firing sequentially as described in section 2.6.2. In order to restrict the spikes to the proper time-window, the shape parameters are chosen so that $\alpha_1 = \cdots = \alpha_{n-1} = r \times 1/n$ and $\alpha_n = 1 - (n-1) \times r/n$, with a common rate parameter of 12Hz. The advantage of this method is that it extends the synaptic inputs over the time-window while preserving the representation of neural spiking as Poisson processes. Note that, in the context of this study, the order in which presynaptic neurons fire is unimportant; only the resulting series of spikes as perceived by the post-synaptic cell matters.

In practice, however, the numerical generation of gamma variates with $\alpha < 1$ is a rather difficult task. Devroye (1986, chap. IX) reviews several interesting algorithms, some of which have been implemented in this project. Unfortunately, when tested, they frequently led to computational problems, almost unavoidable for high number $n$ of synaptic inputs. A subsequent analysis showed that as $n$ increases, $\alpha_{i(i=1\ldots n-1)} \to 0$, and $1/\alpha_i \to \infty$. Although mathematically feasible, this produces computationally out of range (either too big or too small and thus approximated by 0) values for intermediary variables. Consequently, the viability of this technique for the generation of correlated Poisson processes is limited.

Another alternative that has been used in this work is the use of exponential variables instead of gamma for the generation of delays between consecutive neurons. Their rate $\lambda_i = 1/T_i$ is set so that $T_1 = \cdots = T_{n-1} = r \times T_0/n$ ($T_0 = 1/12$) and $T_n = T_0 - (n-1) \times rT_0/n$. This method does not result in Poisson processes for the spiking of each of the artificial neurons, although it guarantees the average frequency of 12Hz and the randomness of spiking. This method is therefore less appealing conceptually than the previous one but nonetheless relevant, because it is unclear how well Poisson processes describe the firing of the cell in the context of an interconnected network. An additional possibility for generating the delay intervals between the artificial neurons is to randomly partition values from an exponential variable into $n$ intervals, among which $(n-1)$ statistically equal.

### 3.3.4 Particular cases

The model of network inputs adopted in this project implicitly assumes correlations between the synaptic events at all levels of synchrony. As mentioned

in section 2.4.1, given the abundant synaptic connections within a network, independent firing of asynchronous presynaptic neurons is, at least, a debatable hypothesis. However, although the approach of desynchronization presented above and the one based on independent inputs are conceptually divergent, they both result in spikes that are statistically equally distributed over time. The equivalence of the two modeling solutions has been verified by comparative tests leading to similar results.

Other simplifications of the synchrony and input models are possible, depending on the particular aspects in focus. A clear example is the initial examination of the effects of $K_A$ on the amplitude of EPSPs. In this case, a simpler representation of inputs through a unique population EPSP seems more suitable to gain the basic understanding aimed at. Therefore, when analyzing the attenuation of EPSPs, either in passive dendrites or in spiking neurons (see section 4.1), only one pulse is delivered through a single synapse. Also, since only the amplitude of the EPSP and its relationship to threshold are observed, increasing synaptic weights could model higher synchrony levels, with no need for changes in time-constants.

# 4 Results and Discussion

This chapter describes and interprets the outcome of the simulations. When relevant, their implications are also discussed. Initially, the role of $K_A$ in excitability regulation is studied in simple contexts with single synaptic inputs. Sections 4.2 to 4.4 examine the effect of $K_A$ on the relationship between the network and the cell for the extreme cases of synchrony and graded levels of it. Finally, we propose hypothetical conditions on Hodgkin-Huxley variables as a possibility of identifying a desynchronizing mechanism involving active currents.

## 4.1 Effects of $K_A$ on excitability

### 4.1.1 Attenuation of propagating EPSPs in passive dendrites

#### Local attenuation for normalized synaptic inputs

First we observe how the EPSP amplitude at the $20^{th}$ compartment is affected by the presence of $K_A$ in the dendrites. This influence is evaluated at increasing strengths of the synaptic input delivered to compartment nr. 30, representing increasing synchrony as commented in section 3.3.4. The effect is analyzed by recording the amplitude of the EPSP without $K_A$ (control conditions) and with $K_A$. The attenuation induced by the presence of $K_A$ is measured as the absolute loss in EPSP amplitude as compared to control conditions.

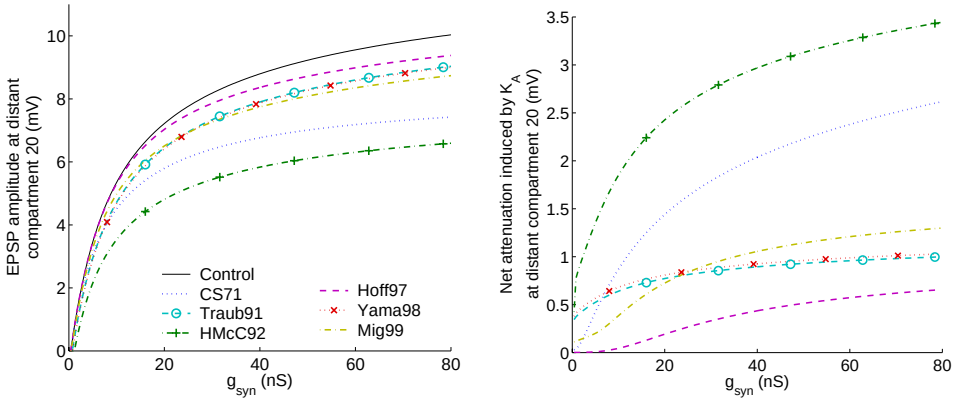


**Figure 4.1:** *[Left] Amplitude of a propagating EPSP at compartment 20. [Right] Loss in amplitude induced by the presence of $K_A$as compared to control conditions ($V_{20}^{Control} - V_{20}^{K_A}$). The parameters are given as a function of the synaptic strength. The legend is common to both graphs.*

These graphs show that, for any input strength, the amplitude of the resulting EPSP is lower with $K_A$ channels than in control conditions. When quantifying this difference in amplitude, we observe that it is larger for stronger inputs and thus, supposedly, for higher synchrony levels among the presynaptic cells.

Since $K_A$ channels are hyperpolarizing, achieving lower depolarizations with them might seem a fully trivial observation. The banality of this result can however be questioned by some other simulations presented below. The two following subsections show some pitfalls that one might fall into when interpreting the expected attenuating effects of $K_A$. The simulations also improve our understanding of the influence of $K_A$ on the amplitude of EPSPs.

### Local attenuation for normalized initial amplitude of EPSPs

Similarly to the previous simulation, we measure the attenuation of the EPSP at compartment 20 as a function of the EPSP amplitude at the input compartment (nr. 30) and not as a function of the synaptic strength (see Figure 4.2).

We observe in this case that, for equal input EPSPs, the presence of the hyperpolarizing current $I_A$ might surprisingly lead to higher amplitudes at distant compartments than with no $K_A$ (*e. g.* Hoff97 in Figure 4.2). In order to interpret this result, it is convenient to reason based on the transfer of charge rather than on currents or potentials, as suggested by Johnston and Wu (1999, p. 406). A given initial EPSP amplitude is associated, in the presence of $K_A$, to higher synaptic conductances than in control conditions. The charge transfer into the dendrite is therefore greater. Consequently, despite the hyperpolarizing properties of the A-channel, the resulting depolarization might be higher with $K_A$. The actual outcome (higher or lower depolarization) probably depends on a delicate balance between the involved synaptic and $K_A$ conductances.

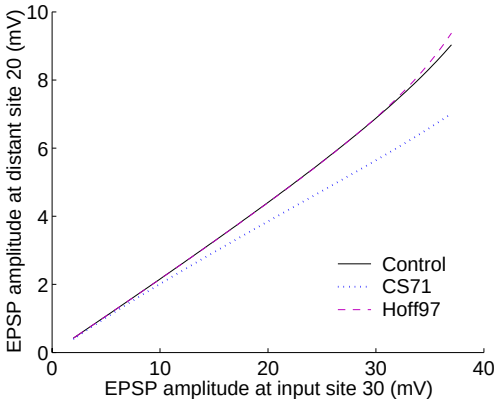


**Figure 4.2:** *Effect of $K_A$ on EPSP amplitude at compartment 20 for identical input depolarizations. Only two $K_A$ channels with opposite effects are represented.*

We conclude that the initial amplitude of the EPSP is a biased criterion for evaluating the effects of $K_A$, which are more objectively measured when taking the same synaptic input as a reference. This choice is consistent with the reasonable assumption that altered neurons that fail to express $K_A$ (*e. g.* heterotopic neurons) conserve their inputs but not their depolarization levels.

### Amplitude decrement along the dendrite

Even when preserving the strength of the synaptic input, the addition of $K_A$ to the passive membrane does not guarantee a stronger attenuation along the

dendrite, *i. e.* a greater peak-voltage decrement between two dendritic points. A check of whether this hypothesis holds has led to the results of Figure 4.3.

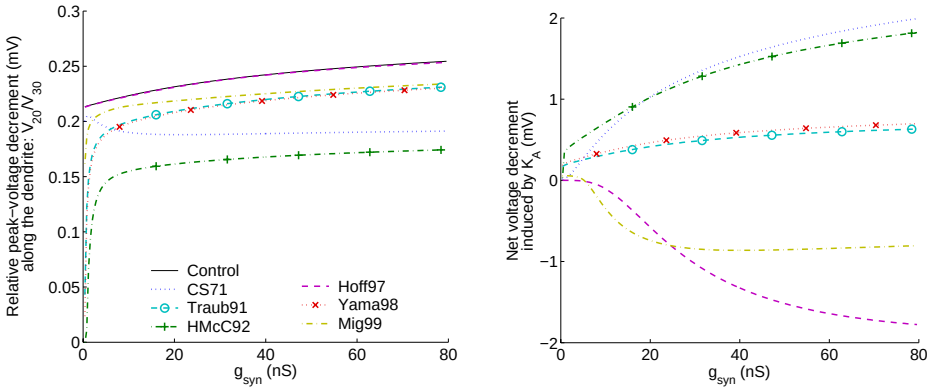


**Figure 4.3:** *Contribution of $K_A$ to the decrement of EPSP-amplitude from input site nr. 30 to distant compartment 20. [Left] Relative peak-voltage between distant and input compartments ($V_{20}/V_{30} \leq 1$) in control conditions and with $K_A$. [Right] Absolute amount of extra peak-voltage decrement induced by $K_A$ as compared to control conditions: $\Delta_V^{K_A} - \Delta_V^{Control}$ with $\Delta_V = V_{input} - V_{distant} \geq 0$. Positive values indicate that the presence of $K_A$ leads to an increased voltage decrement along the dendrite.*

The left graph shows that the relative voltage-decrement obtained in passive dendrites is enhanced by $K_A$ channels, since the ratio $V_{distant}/V_{input}$ is lower with $K_A$. In spite of this, the hyperpolarizing A-current could produce, maybe unexpectedly, a lower absolute decrement along the dendrite than in control conditions, like with Hoff97 and Mig99 (right graph). Lower absolute decrements can be due to the lower local depolarizations obtained with $K_A$ channels, despite the higher rates of relative decrement along the cell. The interplay between the amount of net local attenuation and the amount of relative voltage-decrement along the dendrite probably determines whether $K_A$ contributes to or counteracts the absolute voltage-decrement.

Note that for Hoff97, the result is consistent with that of Hoffman et al. (1997): the relative amount of voltage decrement is similar with or without dendritic voltage-gated channels. Another observation is that most of the relative voltage-decrement along the dendrite is caused by the passive properties of the membrane (75–80% according to Figure 4.3-Left). Furthermore, this value is fairly constant regardless of the strength of the synaptic input.

### $K_A$ effects and synchrony levels: a non-linear dependence?

How the effects of $K_A$ depend on the synaptic strength and hence on the synchrony among presynaptic cells is a complex issue. According to Figure 4.1, inputs of higher synchrony would trigger a stronger action of the A-current, reinforcing the local attenuation of the EPSP. More precisely, the figure showed that this effect is an increasing but sublinear function of $g_{syn}$ (*i. e.* the attenuation increases less rapidly than $g_{syn}$).

However, the concept of linearity has to be manipulated carefully: what is linear or non-linear with respect to what? For instance, a leak current (corresponding

to a constant membrane-conductance) is linear with respect to local membrane potential. However, the addition of leak channels to the membrane results in a higher net attenuation for weak inputs than for strong inputs (sublinear and decreasing function). Therefore, one should not misinterpret the term "linear" and mistakenly infer that a leak current would be more suitable than $K_A$ for counteracting the hypersynchronous states associated to epilepsy.

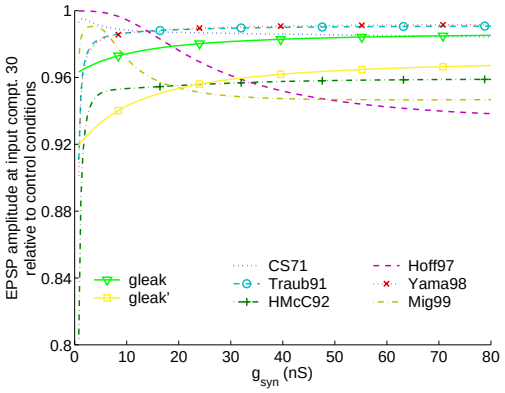


**Figure 4.4:** *Effect of different channels on the local EPSP amplitude at input compartment 20, relative to control amplitude.*

The local attenuation induced by $K_A$ can also be measured by computing the ratio of the EPSP amplitude with $K_A$ to the amplitude in control conditions. Figure 4.4 presents the results at the input compartment ($V_{20}^{K_A}/V_{20}^{Control}$), where the differences among channels are most evident[1]. For comparison purposes, a leak channel has also been considered, with a conductance $g_{leak} = 42.9$ mS.cm$^{-2}$ and $g'_{leak} = 100$ mS.cm$^{-2}$ in two successive simulations.

With leak channels the relative amplitude increases (*i. e.* the local attenuation decreases) with the strength of the synaptic input (*i. e.* with synchrony). On the contrary, $K_A$ channels tend to mitigate this increase or even reverse the tendency, leading to lower relative amplitudes for stronger inputs/synchrony. This inversion becomes significant for channels with rapid activation ($\tau_m$) compared to the duration of the EPSP's rise phase[2] (Hoff97 and Mig99) and/or with a large maximum conductance $\bar{g}_{K_A}$ (CS71) reflecting *e. g.* high channel densities in the membrane.

Consequently, thanks to their rapid kinetics, $K_A$ channels promote an inversion of the EPSP attenuation pattern observed in passive dendrites. A-currents are therefore compatible with the excitability regulation presumed in normal tissue, which reacts to hypersynchronous epileptic states.

It should be emphasized that measuring relative values makes it possible to appreciate dissimilarities between several types of channels, as well as the impact of $K_A$ channels depending on the synchrony among the presynaptic inputs. However, since neural firing is a threshold phenomenon, it is the absolute values of the depolarizations that are most interesting.

### Influence of voltage-shifts and changes in $K_A$ densities and kinetics

In chapter 2 several factors affecting the voltage-dependence of $K_A$ dynamics as well as their density and kinetics have been mentioned (see 2.5.4). Moreover, the descriptions of the dynamics given in Appendix A correspond to certain

[1] the differences are then somewhat "filtered", *i. e.* reduced, along the dendrite.
[2] about 2–2.5 ms at the input site and 5–7 ms at the distant site in our simulations.

experimental conditions. Adjustments might therefore be necessary to account for, for instance, the electrode junction potential and different cell temperatures.

First, we have performed a set of simulations where the dynamics of the different $K_A$ channels ($m$, $h$ and time-constants) have been shifted in voltage. The shift values range from -10mV to +20mV in steps of 5mV. A general conclusion drawn from these simulations is that the effect of a voltage-shift on the strength of the action of $K_A$ can be partly inferred from the position of the $K_A$ normalized conductance curve with respect to the cell's resting potential.

Indeed, in all our simulations (absolute and relative voltage-attenuation, voltage-decrement along the dendrite, etc), the effect of $K_A$ seems to be strengthened when the voltage-shift leads to a larger normalized $K_A$ conductance at rest. For example, with high-voltage activated channels, positive shifts will minimize the effects of $K_A$. On the other hand, successive negative shifts will progressively increase, then maximize and finally reduce the effects of $K_A$, as the normalized conductance curve passes across the resting potential point. The opposite results are to be expected for channels with a range of activation lower than the resting potential. These two opposite cases are well illustrated in Figure 4.5 with Mig99 and Traub91 channels respectively. The graphs show, for different shifts, the absolute extra attenuation at compartment 20 induced by the presence of the $K_A$ channels, similarly to Figure 4.1-Right. Readers are encouraged to refer to the activation curves (especially **g**) in Appendix A (Figure A.1) in order to verify the pertinence of the above interpretation.

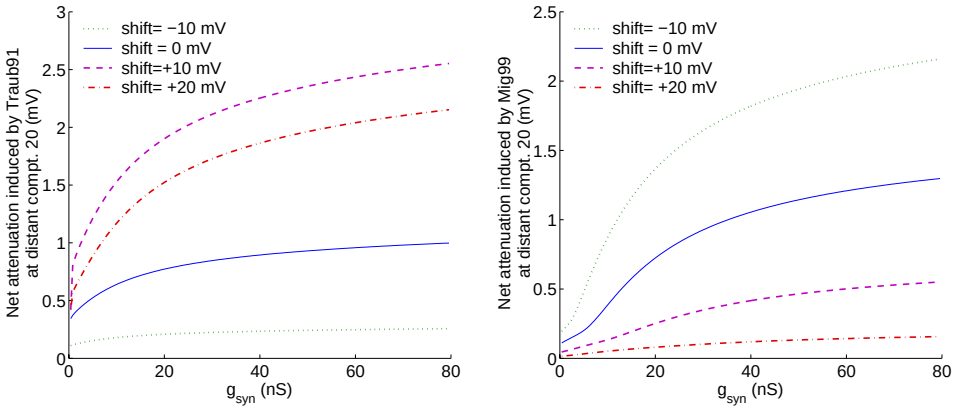


**Figure 4.5:** *Influence of shifts in voltage on the effects of $K_A$ on the local amplitude of EPSPs at distant compartment nr. 20. The graphs show the net (extra) attenuation of the peak-amplitude ($V_{20}^{Control} - V_{20}^{K_A}$) induced by [Left] Traub91 and [Right] Mig99.*

However, an intuitive result is that, in fact, the effect of $K_A$ on EPSP amplitude is not conditioned only by its normalized conductance at rest. The effect should depend as well on the values of $m$ reached with the depolarization by the EPSP, especially for channels with particularly fast activation[3]. In that respect, negative shifts, which favor more substantial activation with the depolarization, should accentuate the effects of $K_A$, and conversely for positive shifts. This phenomenon complicates the simplistic partial interpretation of voltage-shifts

[3]Inactivation operates in general too slowly to significantly influence the effect of $K_A$ on EPSP amplitude.

proposed in the previous paragraph, in which the fast dynamics of $K_A$ channels have not been taken into consideration.

We have consequently tested the influence of changes in A-channel kinetics (time-constants). These changes can be caused by temperature variations or modulators. The simulations account more generally for changes in relative kinetics between $K_A$ and the EPSPs. We have carried out simulations in which the time-constants of $K_A$ have been multiplied by a factor $k$ varying from 0.2 to 2 in steps of 0.2. The results show that, as suggested above, the highest influence of $K_A$ on EPSP amplitude is exerted when, during the rise phase of the EPSP (of duration $T_{rise}$): 1) substantial gains in activation are reached and 2) there is little or no further inactivation. These two conditions ideally imply that $\tau_m \ll T_{rise}$ and $\tau_h \gg T_{rise}$ respectively.

Figure 4.6 provides an explicit illustration of the above comments. The example is based on two channels with relatively slow (CS71) and fast (Mig99) time-constants (see also Figure A.1 in Appendix A) given our "experimental" conditions. The interpretation of the graphs is that when the time-constants become faster (*i. e.* $k$ decreases), the effect of $K_A$ is increased, as long as inactivation remains slower than the EPSP (see CS71, left graph). However, if inactivation is fast enough to operate during the rise phase of the EPSP (Mig99), then slower time-constants (*i. e.* higher $k$) that delay inactivation might make $K_A$ more efficient. The situation would be more complex for channels whose activation and/or inactivation gate has several variants with very different time-constants (like two different inactivation time-constants in HMcC92).

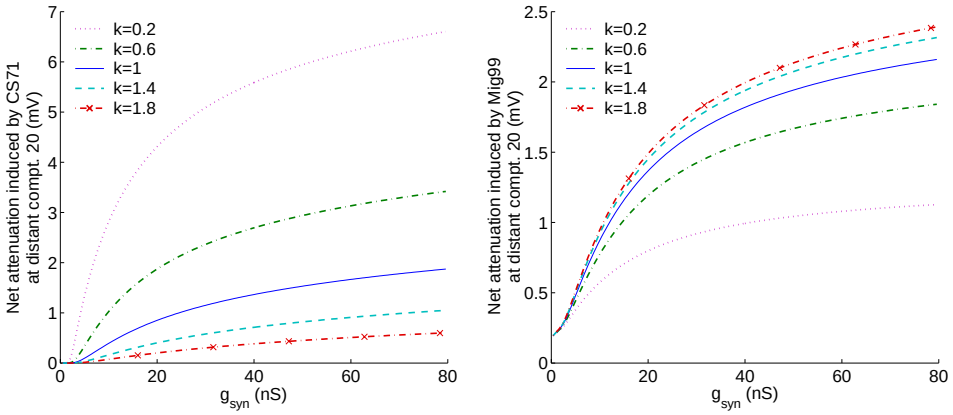


**Figure 4.6:** *Influence of changes in channel kinetics on the attenuation of EPSP amplitude by $K_A$ at distant compartment nr. 20. The graphs show the net (extra) attenuation of the peak-amplitude induced by [Left] CS71 and [Right] Mig99.*

Finally, we have analyzed the effect of changes in the maximum conductance $\bar{g}_{K_A}$. As expected, the results indicate that $\bar{g}_{K_A}$ acts in general similarly to a scaling factor (see equation in Appendix A, p. 45). Decreases or increases of this value respectively mitigate or sharpen each of the variations and differences observed in the simulations, whether they originate from the channel nature, the strength of the synaptic input or from modifications such as voltage-shifts or changes in channel kinetics.

### 4.1.2 Excitability of an active spiking cell

In the following sections we use the model of the active spiking cell presented in section 3.2.3. We thus introduce a spiking threshold and focus on the firing capabilities of the cell. Only the $K_A$ channel Mig99 is analyzed because it is the one originally included in the cell model and because it corresponds to studies in the CA1 region, which is of great interest for instance for epilepsy. Indeed, the experimental conditions in which most of the other mentioned $K_A$ channels were observed differ significantly from those considered in our simulations.

In Figure 4.7 we present a simulation similar to the one shown in Figure 4.1. A synaptic input is delivered at a distal dendrite. The synaptic peak-conductance increases (representing varying synchrony) from 0.8 nS, which is assumed to correspond to a single input, to 400 nS for multiple inputs. We record absolute values of the peak membrane-potential at the soma (left graph). The simulation is repeated for somatic peak-conductances of $K_A$ varying from 0 to 65 mS.cm$^{-2}$, representing modulation of channel densities. The minimum synaptic strength necessary to exceed the spiking potential threshold and thereby produce APs (action potentials) is also plotted as a function of the $K_A$ density (right graph).

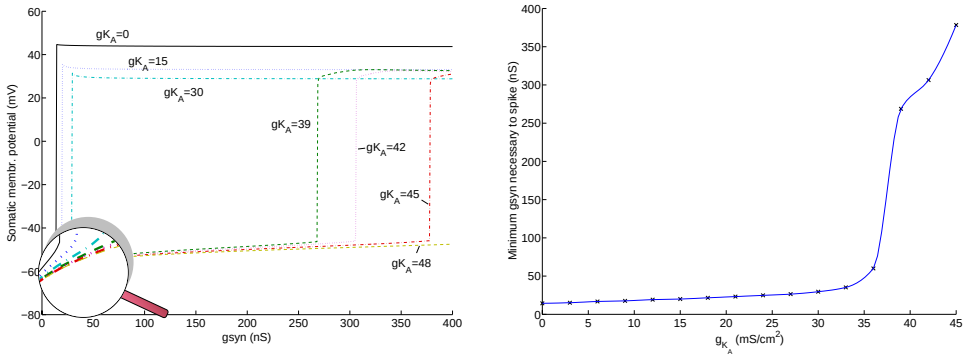


**Figure 4.7:** *Effects of $K_A$ on the excitability of a spiking cell. [Left] Absolute membrane potential at the soma as a function of the synaptic strength for various $K_A$ peak-conductances (in mS.cm$^{-2}$). [Right] Minimum synaptic strength required for firing as a function of the $K_A$ density.*

The curves of peak membrane-potential as a function of $g_{syn}$ (left graph) are downwardly inflected until the firing threshold is reached. This appears very clearly if $g_{syn}$ is limited to 100 nS (graph not shown), but it can also be seen in the current figure through the magnifying lens in the bottom left-hand corner. The observation is consistent with the results obtained in the passive dendrite (see Figure 4.1-Left), despite the pool of active channels present in the current cell model. In the same graph we observe that when $\bar{g}_{K_A}$ changes from 15 to 30, a larger increase in $g_{gsyn}$ is required to spike than when $\bar{g}_{K_A}$ changes from 0 to 15 (larger distance between the vertical sections of the curves). More generally, as $\bar{g}_{K_A}$ is stepped from 0 (no $K_A$) to 65 mS.cm$^{-2}$, it becomes increasingly difficult for the neuron to fire. This is apparently due to the higher net attenuation of strong inputs by $K_A$, combined to the "natural" downward inflection. For high values of $\bar{g}_{K_A}$, none of the considered synaptic strengths drives the neuron over threshold, so no spikes are observed. Note that it is outside the scope of this study to analyze the differences in the peak-amplitudes of spikes.

The graph on the right provides a more accurate representation of how the minimum synaptic strength required for firing varies with changes in $K_A$ densities. It is remarkable that when the $K_A$ density decreases below a certain range, dramatically lower inputs can make the cell fire. In other words, when $K_A$ channels are blocked or poorly expressed, the neuron becomes hyperexcitable. This result seems to confirm the hypotheses formulated by many authors concerning the role of $K_A$ in regulating excitability (see chapter 1 and section 2.4.4). In particular, it is in excellent agreement with the experimental study of Castro et al. (2001) in heterotopic neurons.

We have assumed so far that the network input could be represented by a unique population EPSP whose varying amplitude would model different synchrony levels (see section 3.3.4). This simple representation of inputs has provided a basic understanding of $K_A$ mechanisms. Moreover, the assumption has led to interesting predictions regarding the cell's response depending on the degree of synchrony. However, a main limitation of this approach is that the temporal relationships among the inputs are neglected. Indeed, due to the rapid kinetics of $K_A$, the exact time-course of the membrane depolarization caused by summed EPSPs is expected to have significant implications (see Figure 3.6 in section 3.3.2). Moreover, residual effects from one depolarization might lead to different responses to subsequent identical stimulations, especially if particularly slow mechanisms are present in the membrane.

For example, it is premature and inappropriate to conclude from Figure 4.7-Right that, as the $K_A$ conductance increases, only the highest synchrony levels are capable of (or most efficient in) eliciting APs. Lower synchrony could actually promote $K_A$ inactivation and thereby be more efficient in producing spikes. In the following three sections we look closer into the cell's response at various levels of synchrony with the more detailed model of inputs described in section 3.3. We analyze first the two extreme cases of perfect synchrony and completely asynchronous activity and then intermediate cases.

## 4.2 Cell response to synchronous activity

According to the comments in section 3.3.1, highly synchronous activity implies relatively fast and (very) high-amplitude depolarizations. For this reason, synchrony is known to be extremely efficient in eliciting spikes. $K_A$-currents counteract these depolarizations through rapid activation. However, because $K_A$ also quickly inactivates, its effect is transient, as previously pointed out.

We propose that the fast inactivation of $K_A$ channels enables a more graded control of the cell's response to the excitatory synchronous inputs. Indeed, with no or slow inactivation, the channels' influence on the cell's response is significantly constrained by the amount of activation — the only effective state-variable. In this case, our simulations showed that, through changes in $K_A$ densities, a regulation of the cell's response is possible but rather abrupt, with no progressive change between firing and the avoidance of spikes.

On the contrary, with faster inactivation, the interplay between the two state-variables ($m$ and $h$) should allow a modulation of the transient effect of $K_A$. A

smooth control of the cell's response, particularly of the timing of spikes, becomes possible via $K_A$ modulation (voltage-shifts, densities, temperature, *etc.*), as shown in Figure 4.8. In the simulation we record, for different densities of $K_A$, the membrane potential at two compartments located in a distal dendrite and the soma. One thousand perfectly synchronous inputs are delivered according to the stimulation paradigm explained in section 3.3. It should be noted that, although the three successive synaptic inputs are identical at each simulation, the somatic response is not. This was observed in other simulations as well and confirms the hypothesis of residual effects mentioned in the previous section.

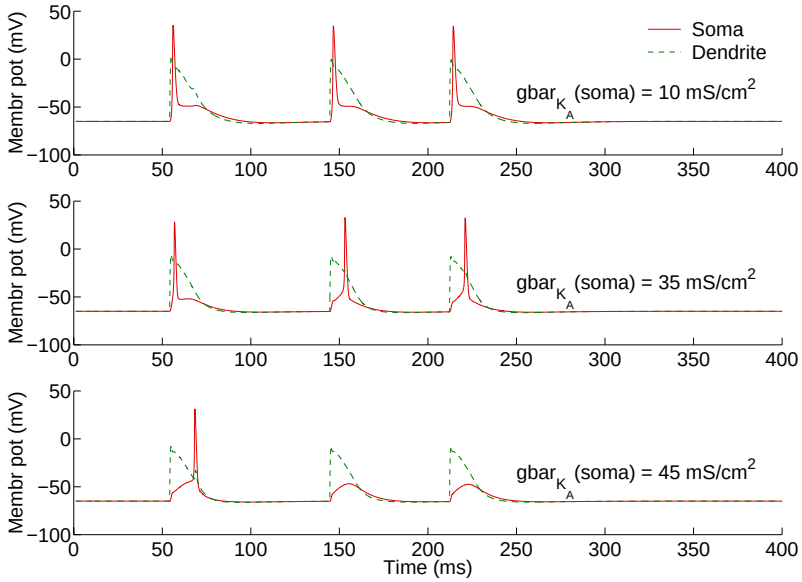


**Figure 4.8:** *Regulation of the cell's response to multiple synchronous inputs by means of $K_A$ modulation. The effect is best seen at the soma. A progressive change between firing and the avoidance of spikes is possible with the fast inactivation of $K_A$. The peak-conductance of $K_A$ at the soma is given as indicative of $K_A$ density.*

Based on these observations and on those on the passive dendrite (see page 27: influence of shifts in voltage), we have derived two intuitive principles intended as tools for anticipating the strength of $K_A$ action under synchronous activity. The prediction is however qualitative (*i. e.* stronger/weaker action), not quantitative, so the exact outcome of the simulation is unknown.

- In general, and especially with slow inactivation, the response is conditioned by the initial level of $K_A$ conductance and by the amount of activation reached at the depolarization levels. Although not rigorous, the following expression can help predict and understand how changes in $K_A$ densities and voltage shifts might influence the cell's response:

$$K_A \text{ effect} \quad \sim \bar{g}_{K_A} \times h^{h_p}(rest) \times m^{m_p}(depol.level)$$

- As inactivation becomes faster, the ratio $\tau_h(depol.level)/T_{EPSP}$ ($T_{EPSP}$ is the duration of the EPSP) plays a more significant role. It is indicative of the amount of inactivation to be expected and of the delaying power of $K_A$. The accuracy of the previous expression is therefore reduced.

Conceptually, the result shows that $K_A$ acts as an intermediary between the high synchrony of the network, which with low $K_A$ densities drives the cells toward firing (see Figure 4.8-Top), and the cellular response. In this case, the relationship can be influenced through modulation of $K_A$, partly as a result of the fast inactivation of the channels.

## 4.3 Cell response to asynchronous activity

As opposed to synchronous activity, asynchronous inputs generate EPSPs whose summation results in low but sustained depolarizations in the neural membrane. Figuratively, for a sufficiently high number of inputs, this should correspond to an electrical DC signal with a superimposed noise causing small fluctuations. Simple simulations with different number of inputs (between 10 and 1000) confirmed this statement. They also indicated that both the DC amplitude and the fluctuating component depend on the total input frequency (*i. e.* the number of inputs times their average frequency) and the time-course of single EPSPs (rise and decay durations). More precisely, decreases in total input frequency and/or faster EPSPs result in a lower DC amplitude with more significant fluctuations around this level. This is illustrated in Figure 4.9 where the somatic membrane-potential variations produced by 10 and 1000 inputs are compared (total input frequencies being then 120 and 1200 Hz respectively).

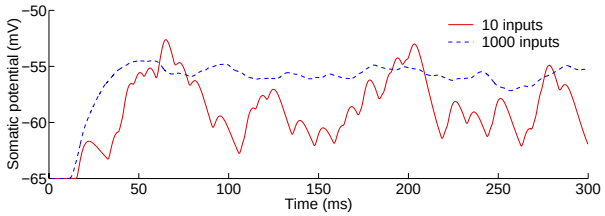


**Figure 4.9:** *Somatic potential in response to the asynchronous activity of 10 and 1000 inputs. Asynchronous activity produces a DC signal with superimposed noisy fluctuations. The relative importance of the two depends on network and cell characteristics.*

Therefore, the presence of asynchronous activity can be thought of as a positive shift of the steady-state point (toward the spiking threshold) that comes with relatively short, smooth and low-amplitude noisy variations. Hence, the firing of the cell relies heavily on both the DC level and the amplitude of the noisy fluctuations. We analyze below the different mechanisms that could affect this response to asynchronous inputs.

Basically, the implication of asynchronous activity for all active currents, including $K_A$, is a change of their normalized conductance as if a new resting-potential had been reached. The DC level is then adapted accordingly, as it occurs also as a result of leak-currents. However, active currents have a better ability to regulate their effect on the DC level, because the value of the normalized conductance around the new resting-potential can be adjusted through changes not only in densities but also in voltage-shifts or kinetics. By adjusting the DC level, it is possible to either enhance or limit the ability of the noisy fluctuations to exceed the firing threshold and produce spikes. However, mainly due to its

fast kinetics, $I_A$ has advantages compared to other currents, among which the ones listed below:

- First, besides its effect on the DC level, $K_A$ has the possibility to control the short noisy fluctuations because of its fast activation. As a result, increases in $K_A$ conductances will not only reduce the DC level but also limit the fluctuations that produce the spikes, thereby reinforcing the decrease in excitability. Conversely, when modulation of $K_A$ leads to lower $K_A$ conductances, there is a more substantial gain in excitability due to the combined effect of a higher DC level and larger noisy fluctuations.
- Second, modifications in $K_A$ conductances are fast, allowing for an "instantaneous" regulation of the cell excitability, whereas other currents require a transition-time until the regulation takes effect.
- Third, there is a very diverse and rich assortment of mechanisms allowing for $K_A$ modulation and thereby for controlling the amount of A-current around the new-state point (see section 2.5.4).

Figure 4.10 shows an example in which voltage-shifts of $K_A$ dynamics enable a control of the cell's firing response. The somatic potential produced by 1000 asynchronous inputs is recorded for four different voltage-shifts. With only 10 inputs we obtained similar results. However, since the DC level is then lower, larger $K_A$ changes are required to affect the cell response, but the changes in excitability are more progressive due to the larger fluctuations[4].

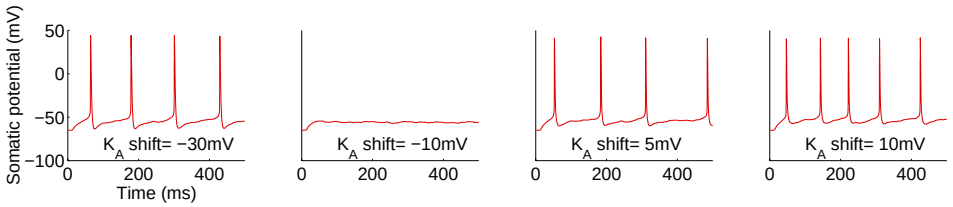


**Figure 4.10:** *Regulation of cell excitability through voltage-shifts of $K_A$ dynamics with 1000 asynchronous inputs. The latter produce a constant depolarization that changes the steady-state point; the modulation of $K_A$ then determines the amount of $K_A$ conductance around this new working point.*

The results reveal that, as the voltage-shift increases, the excitability is first decreased and then restored. We interpret this as the direct consequence of the previous comments: the modulation of $K_A$ modifies the amount of A-current around the potentials reached with the DC signal. In this case, the asynchronous inputs produce, after summation, a depolarization around $V_{dc} = -48$ mV in distal dendrites and -55 mV at the soma. Voltage-shifts of $K_A$ have the effect of translating the curve of the steady-state normalized conductance $\mathbf{g}$, thereby changing the value of this conductance around the potential $V_{dc}$, as indicated in Figure 4.11. The bell-shaped form of the curve explains then the evolution of the excitability observed in Figure 4.10 for progressive voltage-shifts of $K_A$. Thus, with asynchronous activity, the curve of the steady-state normalized conductance represents a valuable tool for anticipating the possible effects of $K_A$ on excitability.

[4] it becomes easier to adapt the number of times that the firing threshold is exceeded.

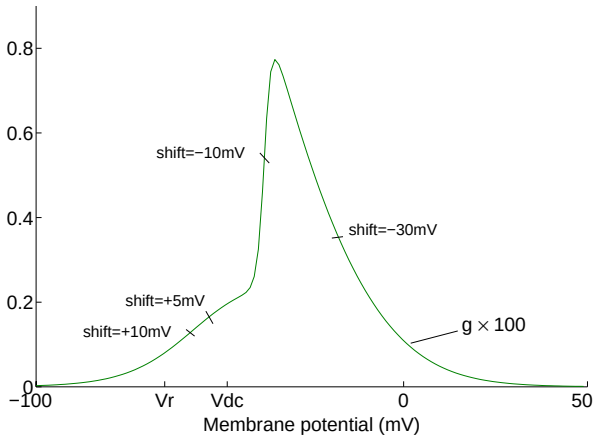


**Figure 4.11:** *Influence that several voltage-shifts would have on the amount of normalized conductance of $K_A$ obtained at $V_{dc}$, the potential reached with the sustained depolarization caused by asynchronous activity. The resting potential is noted $V_r$.*

Our simulations indicate that $K_A$ is also capable of modifying the relationship between asynchronous network inputs and the cell's excitability and firing response. Although other currents might play a similar role, higher efficiency is to be expected with $K_A$. Indeed, the modulation and rapidity of $K_A$ confer to these channels interesting means of mediating between the network and the neuron. It is important to emphasize however that the mechanisms of this mediation differ fundamentally from those involved in synchronous activity.

## 4.4 Cell response to graded degrees of synchrony

In the previous sections we have investigated how $K_A$ influences the relationships between the network and individual neurons at two extreme levels of synchrony. The simulations showed that different mechanisms allow for regulation of this coupling. As part of an extension of these results, in this section we analyze the trilateral relationship between the network, $K_A$ and the cell firing for graded levels of synchrony.

It can be presumed that such a relationship at intermediate degrees of synchrony results from a compromise between the effects of the DC depolarization level observed with asynchronous inputs and those of the large, short fluctuations caused by synchronous activity. In addition, the high-frequency variations among the inputs[5] (see Figure 3.6 in section 3.3.2) are also likely to affect the relationship. However, it is not intended to explore the mechanisms that underlie these relationships, but rather to infer the complex interplay that might take place in a fully interconnected network and the role of $K_A$ as a possible regulatory mechanism.

In the next simulation we analyze the firing of a cell receiving inputs from a network with varying synchrony levels. We mimic this network input of progressive synchrony (from 0 to 100%) according to the modeling scheme presented

[5]and therefore the relationship between the number of inputs, their frequency and the exact time-course of the EPSPs

in section 3.3. In this case we consider 10 inputs, each having a frequency of 12 Hz, and simulations are run for 1500 ms. $K_A$ densities are increased from 0 to 60 mS.cm$^{-2}$ as the peak value at the soma. The results are presented in the 3D-plot of Figure 4.12.

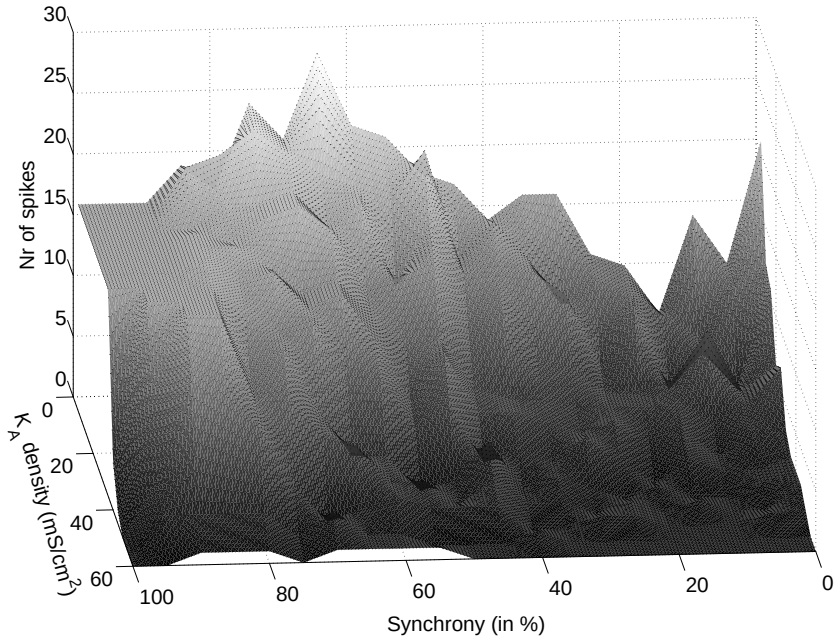


**Figure 4.12:** *Cellular firing response to graded degrees of synchrony in the network. Synchrony increases from right to left from 0% (asynchronous activity) to 100% (perfect synchrony), $K_A$ densities between 0 and 60 mS.cm$^{-2}$.*

This result gives rise to many interesting interpretations. For any fixed degree of synchrony, the conclusion is that the excitability decreases as $K_A$ densities increase. This observation was to be expected, since $K_A$ acts by attenuating absolute potentials. However, the effect of $K_A$ on excitability varies considerably at different levels of synchrony, leading to complex relationships between synchrony and excitability.

Indeed, both the steepness and the amplitude of excitability changes due to $K_A$ modulation are synchrony-dependent. The change in excitability with $K_A$ modulation seems to become more abrupt as synchrony increases, resulting in a "binary" response (many spikes or almost none) for highly synchronous activity. Concerning the amplitude of the change, the largest excitability variations are observed with very asynchronous activity and with synchrony levels between 60 and 80%. The smallest changes in excitability occur around 20% of synchrony. However, as mentioned above, the explanation of such irregular changes is currently beyond the scope of this work.

The previous observations indicate that, due to the action of $K_A$, excitability and synchrony are not trivially related to each other. For "normal" density values[6] of $K_A$ (30–50 mS.cm$^{-2}$), the largely accepted idea of highest synchrony being most effective in producing spikes holds. However, modulation in $K_A$

[6]The model was originally set up to reproduce a standard electrophysiological behavior.

densities can make lower synchrony states much more prone to excitability, or even hyperexcitable. For example, with significantly asynchronous inputs (∼0% synchrony), blockade of the A-current or failure to express it can result in substantial firing levels (see previous section).

As mentioned above, the exact outcome of the simulation and thus the trilateral relationship may change significantly depending on, among others, the total number of inputs, their average frequency, the exact time-course of single EPSPs, the properties of the membrane (time-constant) and the dynamics of the considered $K_A$ channel. In spite of that, the results seem to confirm that $K_A$ provides a means of altering the trivial relationship between synchrony levels in the network and cellular excitability. Furthermore, assuming that there are other mechanisms imposing the firing frequency of the cell, we suggest that $K_A$ can constrain the synchrony levels in the network of the activity to which the neuron tends to participate.

## 4.5 Intrinsic desynchronizing dendritic mechanism

The ability of A-channels to counteract (delay, reduce or even suppress) high and fast depolarizations —as a consequence of its fast kinetics— is one of its most well-known characteristics. Such depolarizations are typical with synchronous activity. However, our previous simulations have revealed that, because $K_A$ is so fast and so active around slightly depolarized potentials with respect to rest, it also has significant effects on asynchronous activity.

Asynchronous activity is believed to be necessary to several mental processes and in particular to working memory tasks (Compte et al., 2003). However, the intact nervous system presumably possesses also mechanisms avoiding hypersynchronous activity in order to prevent, for example, epilepsy.

We have therefore investigated the existence of so-called desynchronizing mechanisms that would prevent neurons from participating in highly synchronous activity without affecting asynchronous inputs. This possibility has been analyzed, of course, based on the previously acquired understanding of how $K_A$ operates at several degrees of synchrony. We focus thus on desynchronization through dendritic active currents described by Hodgkin-Huxley dynamics.

Our reflection has aimed at finding Hodgkin-Huxley dynamics that would lead to the desired effect, departing from one of the studied $K_A$ channels, namely Mig99. The suggested modifications of the dynamics could be obtained via phosphorylation and other modulation systems presented in section 2.5.4. We assume a sufficiently high number of inputs so that asynchronous activity results in a sustained depolarization called DC signal (see section 4.3 and Figure 4.9) and not in isolated EPSPs. As a result of our analysis, we propose below a set of hypothetical conditions on these variables. We note $V_{rest}$ the *in vivo* resting-potential, $V_A$ the steady potential for asynchronous inputs ($V_A \equiv V_{rest} + DC$) and $V_S$ the steady potential for synchronous activity ($V_S \approx V_{rest}$)

- The normalized conductance peak should preferably be located close to $V_{rest}$. This produces a significant hyperpolarizing current at $V_S$ that will counteract the synchronous inputs, but not necessarily at $V_A > V_S$.

- A steep inactivation curve, so that $h_\infty^{hp} \approx 1$ around $V_S$ and $h_\infty^{hp} \approx 0$ around $V_A$, *i. e.* at slightly depolarized potentials with respect to rest. Since the fast and high depolarizations of synchronous activity result in a significant instantaneous activation ($m \to 1$ very quickly), the normalized conductance will be maximized in response to synchronous inputs ($g = h_\infty^{hp}(V_S) \times m^{mp}(\mathit{depol}) \approx 1$). On the contrary, with asynchronous activity, the resulting sustained depolarization will inactivate the channels, thereby neutralizing their effect.

- A smooth activation curve. With this we achieve the following compromise: to limit the steady-state activation value at $V_A$, while enabling a significant amount of activation at $V_S$ (see first condition). Together with the previous condition, this decreases even further the normalized conductance at the depolarization level created by asynchronous activity ($g = h_\infty^{hp}(V_A) \times m_\infty^{mp}(V_A) \approx 0$). The consequences of this condition on synchronous activity should be negligible, since in this case the channels quickly activate.

- Fast inactivation (small $\tau_h$) at $V_A$, but much slower at highly depolarized potentials. This condition ensures that $h$ is rapidly decreased with small depolarizations so that the effect of the channels on single inputs or asynchronous activity is limited. It also avoids inactivation of the channels with the high depolarizations produced by synchronous inputs.

- Slow activation (small $\tau_m$) at $V_A$, but much faster at highly depolarized potentials. The reason for this condition is symmetrical to the that of the previous one.

Additional conditions might be necessary in order to obtain dendritic desynchronizing mechanisms. Also, some of the suggested ones might not have a significant impact, although all of them should contribute to some extent to achieve desynchronization. Assuming the existence of such desynchronizing currents, they would have little or no impact on asynchronous activity. Conversely, participation of the neuron to synchronous activity would require for instance blockade of the channels. Consequently, modulation of the current would also play a very critical role in controlling the interaction between the network and the neuron.

*This page intentionally left blank*

# 5 Conclusions

As a general conclusion, this work has revealed that $K_A$ channels provide mechanisms to alter the interaction between individual neurons and neural networks. We deduce that A-currents have a certain ability to influence the functioning of the brain. More precisely, we have shown that the commonly assumed trivial relationship between network synchrony and cellular firing can be modified in complex ways through modulation of $K_A$.

Our modeling efforts suggest that, in the context of this project, synchrony should be defined post-synaptically and not based on firing correlations. In particular, we propose that synchrony can be represented as the average time-window of EPSP summation. We also establish the modeling necessity in studies of synchrony to consider multiple synaptic inputs rather than smooth population synaptic inputs.

The simulations on the passive dendrite demonstrate that the attenuating effect of $K_A$ on EPSP-amplitude has to be interpreted in terms of local absolute potentials resulting from inputs of identical synaptic strength. Interpretations in terms of peak-voltage decrement along the dendrite or assuming initially identical EPSP amplitudes have been proven erroneous. We also point out the necessity of comparing absolute rather than relative values, since firing is a threshold phenomenon. In spite of that, relative values (with and without $K_A$) are helpful for comparisons among channels and for understanding how they operate in response to several synaptic strengths. In that respect, the attenuation by $K_A$ is larger for stronger synaptic inputs, although the increase is sublinear. Furthermore, A-currents provide a control against the hyperexcitability promoted by strong inputs, such as those resulting from highly synchronous activity. Also, failure to express the A-current in an active cell leads to dramatic increases in excitability. We argue in addition that the regulation of $K_A$ channels through their multiple modulatory mechanisms plays a decisive role in the relationship between the network inputs and the cellular excitability.

With perfectly synchronous activity, $K_A$ is able to affect the timing of the firing response or even suppress it. Partly due to the fast inactivation, modulation of $K_A$ modifies its transient effect and thereby the interplay between the network and the neuron. Highly asynchronous activity gives rise to a sustained depolarization with superimposed noise. Modulation of $K_A$ enables in this context a combined regulation of the two consequences, which alters the cell's firing response. The two extreme cases of synchrony imply thus a role of $K_A$ in regulating the interaction between the network and the cell, although through different mechanisms. In each of these cases, we propose methods for anticipating to

some extent the influence of changes in $K_A$. All levels of synchrony considered, the conclusion is that both the amplitude and the steepness of changes in excitability (measured in number of spikes) induced via $K_A$ modulation are different at different degrees of synchrony. Because of these differences, cell firing and network synchrony are not trivially related to each other. Instead, their relationship depends heavily on $K_A$ and its modulating mechanisms. As a result, we argue that studies focused on the response of a cell in a network and more particularly studies of synchrony should not neglect this interdependence.

Finally, from the acquired understanding of the functioning and influence of $K_A$, we infer the possibility of preventing synchronous activity by means of active dendritic currents with specific Hodgkin-Huxley dynamics. We believe that the identification of such desynchronizing mechanisms could represent a significant asset for future research in several areas of neuroscience.

Possible further research as an extension to this work includes the following suggestions:

- Experimental work to compare the outcome with the conclusions obtained in this computational study;
- Validation of the hypothetical conditions on Hodgkin-Huxley variables for preventing synchrony, either theoretically with a fictitious channel or with an existing channel satisfying the listed requirements;
- Deeper analysis and understanding of the mechanisms underlying the irregularities observed at intermediate levels of synchrony;
- Study of and comparison with other currents that could also mediate between the network and the neuron, such as $I_D$ or $I_h$.

# References


Akins, P. T., Surmeier, D. J., and Kitai, S. T. (1990). Muscarinic modulation of a transient $K^+$ conductance in rat neostriatal neurons. *Nature*, 344(6263):240–242.

Baker, S., Kilner, J., Pinches, E., and Lemon, R. (1999). The role of synchrony and oscillations in the motor output. *Experimental Brain Research*, 128(1-2):109–117.

Bower, J. M. and Beeman, D. (1994). *The Book of GENESIS: Exploring Realistic Neural Models with the GEneral NEural SImulation System.* TELOS, Springer-Verlag, Santa Clara, CA, 1st edition.

Brody, C. D. (1999). Correlations without synchrony. *Neural Computation*, 11:1537–1551.

Bush, P. C. and Sejnowski, T. J. (1993). Reduced compartmental models of neocortical pyramidal cells. *Journal of Neuroscience Methods*, 46(2):159–166.

Castro, P. A., Cooper, E. C., Lowenstein, D. H., and Baraban, S. C. (2001). Hippocampal heterotopia lack functional Kv4.2 potassium channels in the methylazoxymethanol model of cortical malformations and epilepsy. *The Journal of Neuroscience*, 21(17):6626–6634.

Coetzee, W., Amarillo, Y., Chiu, J., Chow, A., Lau, D., McCormack, T., Moreno, H., Nadal, M., Ozaita, A., Pountney, D., Saganich, M., Vega-Saenz de Miera, E., and Rudy, B. (1999). Molecular diversity of K+ channels. *Ann. N.Y. Acad. Sci.*, 868:233–285.

Compte, A., Constantinidis, C., Tegner, J., Raghavachari, S., Chafee, M. V., Goldman-Rakic, P., and Wang, X. J. (2003). Temporally irregular mnemonic persistent activity in prefrontal neurons of monkeys during a delayed response task. *Journal of Neurophysiology.* E-publication ahead of print.

Connor, J. A. and Stevens, C. F. (1971). Prediction of repetitive firing behaviour from voltage clamp data on an isolated neurone soma. *Journal of Physiology*, 213(1):31–53.

Devroye, L. (1986). *Non-Uniform Random Variate Generation.* Springer-Verlag, New York.

Engel, A. K., Fries, P., and Singer, W. (2001). Dynamic predictions: Oscillations and synchrony in top-down processing. *Nature Reviews Neuroscience*, 2(10):704–716.

Eriksson, D. (2002). Simulation of synaptic plasticity and its contribution to the dynamics in a cortical microcircuit. Master's Thesis TRITA-NA-E02068, Royal Institute of Technology of Stockholm (KTH).

Hebb, D. (1949). *The Organization of Behavior: A Neuropsychological Theory*. Wiley, New York.

Hess, D. and El Manira, A. (2001). Characterization of a high-voltage-activated $I_A$ current with a role in spike timing and locomotor pattern generation. *Proc. Natl. Acad. Sci. USA*, 98(9):5276–5281.

Hines, M. L. and Carnevale, N. T. (1997). The NEURON simulation environment. *Neural Computation*, 9(6):1179–1209.

Hodgkin, A. L. and Huxley, A. F. (1952). A quantitative description of membrane current and its application to conduction and excitation in nerve. *Journal of Physiology*, 117:500–544.

Hoffman, D. A., Magee, J. C., Colbert, C. M., and Johnston, D. (1997). $K^+$ channel regulation of signal propagation in dendrites of hippocampal pyramidal neurons. *Nature*, 387(6636):869–875.

Huguenard, J. R. and McCormick, D. A. (1992). Simulation of the currents involved in rhythmic oscillations in thalamic relay neurons. *Journal of Neurophysiology*, 68(4):1373–1383.

Johnston, D., Hoffman, D. A., Magee, J. C., Poolos, N. P., Watanabe, S., Colbert, C. M., and Migliore, M. (2000a). Dendritic potassium channels in hippocampal pyramidal neurons. *Journal of Physiology*, 525:75–81.

Johnston, D., Hoffman, D. A., and Poolos, N. P. (2000b). Potassium channels and dendritic function in hippocampal pyramidal neurons. *Epilepsia*, 41(8):1072–1073.

Johnston, D. and Wu, S. (1999). *Foundations of Cellular Neurophysiology*. The MIT Press, Cambridge, 4th edition.

Kandel, E. R., Schwartz, J. H., and Jessel, T. M. (2000). *Principles of Neural Science*. McGraw-Hill, USA, 4th edition.

Koch, C. and Segev, I. (1998). *Methods in Neuronal Modeling*. The MIT Press, Cambridge, 2nd edition.

Llinás, R., Leznik, E., and Urbano, F. J. (2002). Temporal binding via cortical coincidence detection of specific and nonspecific thalamocortical inputs: a voltage-dependent dye-imaging study in mouse brain slices. *Proc. Natl. Acad. Sci. USA*, 99(1):449–454.

Lytton, W. W. and Sejnowski, T. J. (1991). Simulations of cortical pyramidal neurons synchronized by inhibitory interneurons. *Journal of Neurophysiology*, 66(3):1059–1079.

Magee, J. C. and Cook, E. P. (2000). Somatic EPSP amplitude is independent of synapse location in hippocampal pyramidal neurons. *Nature Neuroscience*, 3(9):895–903.

Migliore, M., Hoffman, D. A., Magee, J. C., and Johnston, D. (1999). Role of an A-type $K^+$ conductance in the back-propagation of action potentials in the dendrites of hippocampal pyramidal neurons. *Journal of Computational Neuroscience*, 7(1):5–15.

Poirazi, P., Brannon, T., and Mel, B. W. (2003). Arithmetic of subthreshold synaptic summation in a model CA1 pyramidal cell. *Neuron*, 37(6):977–987.

Poolos, N. P., Migliore, M., and Johnston, D. (2002). Pharmacological upregulation of h-channels reduces the excitability of pyramidal neuron dendrites. *Nature Neuroscience*, 5(8):767–774.

Pyapali, G. K., Sik, A., Penttonen, M., Buzsaki, G., and Turner, D. A. (1998). Dendritic properties of hippocampal CA1 pyramidal neurons in the rat: Intracellular staining in vivo and in vitro. *Journal of Comparative Neurology*, 391(3):335–352.

Saint, D. A., Thomas, T., and Gage, P. W. (1990). GABAB agonists modulate a transient potassium current in cultured mammalian hippocampal neurons. *Neurosci. Lett.*, 118(1):9–13.

Singer, W. (1999). Neuronal synchrony: a versatile code for the definition of relations? *Neuron*, 24(1):49–65.

Singer, W. (2003). Personal communication. e-mail. On reply to Erik Fransén.

Svennenfors, B. (2003). Population effects on the dynamics of a cortical network of pyramidal cells and FSN interneuron. Master's thesis, Royal Institute of Technology of Stockholm (KTH). In print.

Traub, R. D., Wong, R. K. S., Miles, R., and Michelson, H. (1991). A model of a CA3 hippocampal pyramidal neuron incorporating voltage-clamp data on intrinsic conductances. *Journal of Neurophysiology*, 66(2):635–650.

Yamada, W. M., Koch, C., and Adams, P. R. (1998). Multiple channels and calcium dynamics. In Koch, C. and Segev, I., editors, *Methods in Neuronal Modeling: From Ions to Networks*, chapter 4, pages 137–170. The MIT Press, Cambridge.

Zona, C., Tancredi, V., Longone, P., D'Arcangelo, G., D'Antuono, M., Manfredi, M., and Avoli, M. (2002). Neocortical potassium currents are enhanced by the antiepileptic drug lamotrigine. *Epilepsia*, 43(7):685–690.

# Appendix A – $K_A$ dynamics

The dynamics of the channels are expressed either by $\alpha_y(V)$ and $\beta_y(V)$ (with $y \equiv m, h$) or by $y_\infty(V)$ and $\tau_y(V)$. Except for CS71 (see Table A.1), mathematical expressions are derived via interpolation from the experimental data. For all channels, the state variables, normalized conductance and time-constants are plotted in page 48, Figure A.1. In general terms, the A-current is given by:

$$I_A = \bar{g}_A m^{m_p} h^{h_p} (V - E_K) \qquad \text{where} \begin{cases} E_K = \frac{RT}{F} \log \frac{[K^+]_{out}}{[K^+]_{in}} \\ R = 1.987 \text{ cal/mol-}^\circ K \\ F = 9.648 \times 10^4 \text{ C/mol}, \quad T \text{ in } ^\circ K \end{cases}$$

• **Connor and Stevens, 1971: CS71.**

**Table A.1** Experimental values for dynamics of CS71.

| $V(mV)$ | $\alpha_m(s^{-1})$ | $\beta_m(s^{-1})$ | $\alpha_h(s^{-1})$ | $\beta_h(s^{-1})$ |
|---|---|---|---|---|
| -100 | 0.0 | 83.3 | 4.26 | 0.00 |
| -95 | 0.0 | 83.3 | 4.12 | 0.13 |
| -90 | | | 3.95 | 0.31 |
| -85 | | | 3.69 | 0.57 |
| -80 | ⋮ | ⋮ | 3.34 | 0.92 |
| -75 | | | 2.94 | 1.32 |
| -70 | | | 2.32 | 1.93 |
| -65 | 0.0 | 83.3 | 1.54 | 2.72 |
| -60 | 0.1 | 83.2 | 0.66 | 3.60 |
| -55 | 20.8 | 62.6 | 0.31 | 3.95 |
| -50 | 38.4 | 44.9 | 0.12 | 4.13 |
| -45 | 47.2 | 36.2 | 0.05 | 4.20 |
| -40 | 54.3 | 29.1 | 0.00 | 4.26 |
| -35 | 60.8 | 22.6 | 0.00 | 4.26 |
| -30 | 65.7 | 17.7 | | |
| -25 | 71.0 | 12.3 | | |
| -20 | 74.8 | 8.5 | | |
| -15 | 78.0 | 5.0 | ⋮ | ⋮ |
| -10 | 80.0 | 3.1 | | |
| -5 | 83.0 | 1.2 | | |
| 0 | 83.3 | 0.0 | 0.00 | 4.26 |
| ⋮ | ⋮ | ⋮ | ⋮ | ⋮ |
| 50 | 83.3 | 0.0 | 0.00 | 4.26 |

**• Traub *et al.* , 1991: Traub91**

$$\alpha_m = \frac{20(13.1 - V)}{-1 + e^{(13.1-V)/10}}$$
$$\beta_m = \frac{17.5(V - 40.1)}{-1 + e^{(V-40.1)/10}}$$
$$\alpha_h = 1.6e^{-(V+13)/18}$$
$$\beta_h = \frac{50}{1 + e^{(10.1-V)/5}}$$

Voltages are in mV, $\alpha_y$ and $\beta_y$ ($y \equiv m, h$) in ms$^{-1}$.

**• Huguenard and McCormick, 1992: HMcC92**

In this case, the $I_A$ current has been differentiated into two components, $I_{A1}$ and $I_{A2}$, because a simple Boltzmann curve could not be well fitted to the experimental data due *e. g.* to the biexponential time-course of inactivation. $I_{A1}$ accounts for 60% of the total $I_A$ conductance. Voltages in mV, times in ms.

$$m_\infty^{A1} = \frac{1}{1 + e^{-(V+60)/8.5}}$$
$$m_\infty^{A2} = \frac{1}{1 + e^{-(V+36)/20}}$$
$$\tau_m^{A1} = \tau_m^{A2} = \frac{1}{e^{(V+35.8)/19.7} + e^{-(V+79.7)/12.7}} + 0.37$$
$$h_\infty^{A1} = h_\infty^{A2} = \frac{1}{1 + e^{(V+78)/6}}$$

Then, with $\tau_0 = \frac{1}{e^{(V+46)/5} + e^{-(V+238)/37.5}}$

$$\tau_h^{A1} = \begin{cases} \tau_0 & \text{if } V < -63mV \\ 19ms & \text{if } V \geq -63mV \end{cases}$$
$$\tau_h^{A2} = \begin{cases} \tau_0 & \text{if } V < -73mV \\ 60ms & \text{if } V \geq -73mV \end{cases}$$

**• Hoffman *et al.* , 1997: Hoff97**

Hoffman *et al.* make a distinction between proximal ($\leq$100 $\mu$m from soma) and distal ($>$100 $\mu$m) channels: the activation curve for the later has a relative negative shift and a slightly different slope.

$$m_\infty = \frac{1}{1 + e^{-(V(mV)-V_{1/2})/k}} \quad \text{with} \quad \begin{cases} V_{1/2}^{prox} = +11mV, & k_{prox} = 18 \\ V_{1/2}^{dist} = -1mV, & k_{dist} = 15 \end{cases}$$
$$\tau_m = 0.2ms$$
$$h_\infty = \frac{1}{1 + e^{(V(mV)+56)/8}}$$
$$\tau_h = \begin{cases} 5ms & \text{if } V < -20mV \\ 5 + 0.26(V(mV) + 20)ms & \text{if } V \geq -20mV \end{cases}$$

• **Yamada *et al.* , 1998: Yama98**

$$m_\infty = \frac{1}{1+e^{-(V(mV)+42)/13}}$$

$$\tau_m = 1.38ms$$

$$h_\infty = \frac{1}{1+e^{(V(mV)+110)/18}}$$

$$\tau_h = \begin{cases} 50ms & \text{if } V < -80mV \\ 150ms & \text{if } V \geq -80mV \end{cases}$$

• **Migliore *et al.* , 1999: Mig99**

The same distinction between proximal and distal channels done by Hoffman *et al.* is made in this case. The expressions of steady-state activation and inactivation and of time-constants depend on intermediary variables. Voltages are considered to be in mV and times in ms.

$$a_m^{prox} = \exp\left[-0.038\left(1.5 + \frac{1}{1+\frac{1}{5}\exp(V+40)}\right)(V-11)\right]$$

$$b_m^{prox} = 4\exp\left[-0.038\left(0.825 + \frac{1}{1+\frac{1}{5}\exp(V+40)}\right)(V-11)\right]$$

$$a_m^{dist} = \exp\left[-0.038\left(1.8 + \frac{1}{1+\frac{1}{5}\exp(V+40)}\right)(V+1)\right]$$

$$b_m^{dist} = 2\exp\left[-0.038\left(0.7 + \frac{1}{1+\frac{1}{5}\exp(V+40)}\right)(V+1)\right]$$

Then the dynamics of the channel are defined by:

$$m_\infty = \frac{1}{1+a_m}$$

$$\tau_m = \max\left(0.1, \frac{b_m}{1+a_m}\right)$$

$$h_\infty = \frac{1}{1+e^{0.11(V+56)}}$$

$$\tau_h = \max\left(2, 0.26(V+50)\right)$$

• **Graphical representation for all channels**

The dynamics of the six channels described above are represented in Figure A.1. The graphs show the voltage-dependence of the steady-state activation, inactivation and normalized conductance as well as that of the time-constants.

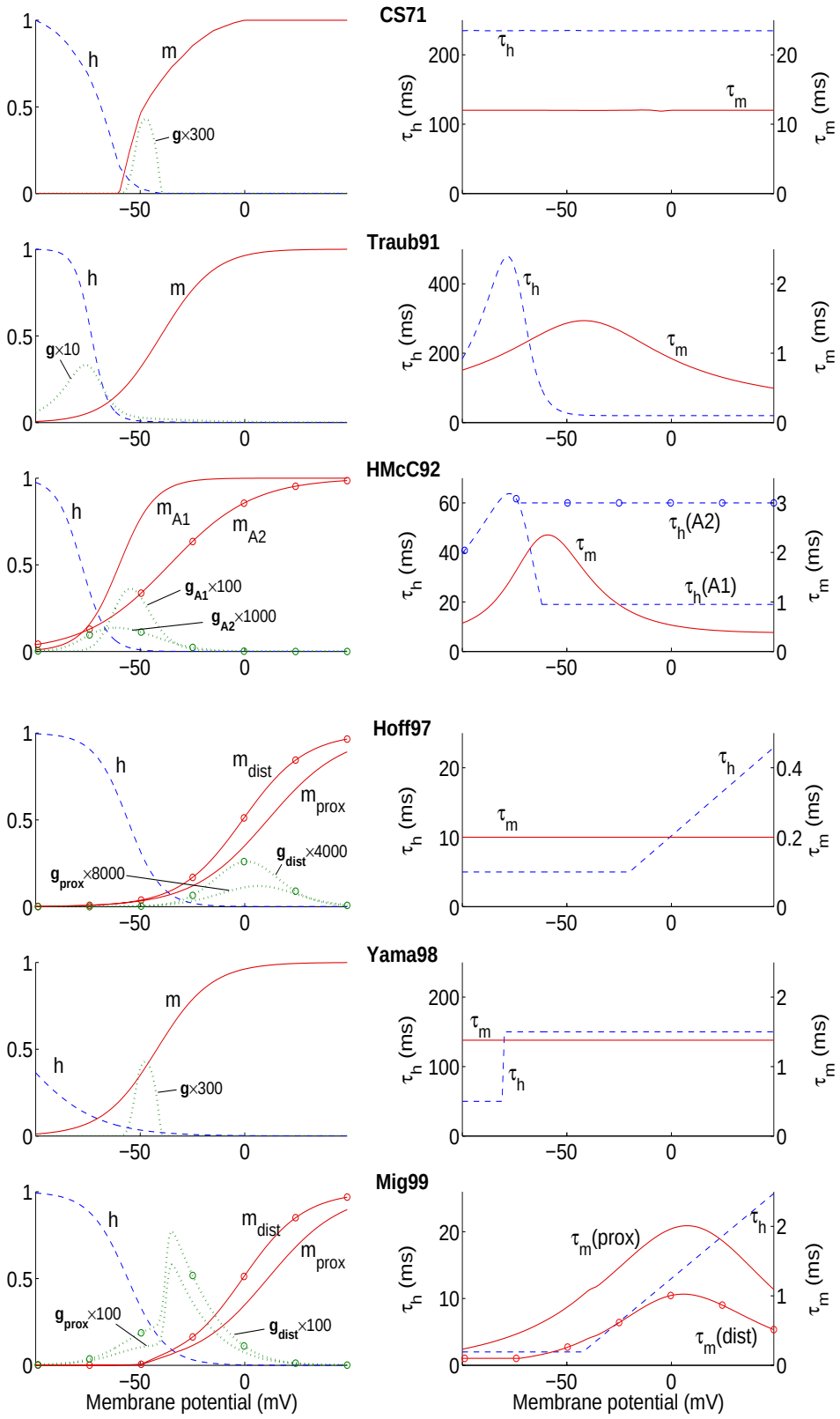


**Figure A.1:** *Dynamics of the six $K_A$ channels: [Left] Steady-state activation ($m$), inactivation ($h$) and normalized conductance ($\mathbf{g}$) and [Right] time-constants. Note the changes in scale for the time-constants.*

# Appendix B – Synaptic conductance changes

Synaptic conductance changes are described by means of analytical functions. The "alpha function" offers a good approximation of these changes (see Figure B.1):

$$g_{syn}(t) = g_{max}\frac{t}{\tau_{syn}}\exp(1 - t/\tau_{syn})$$

This function peaks at $t = \tau_{syn}$ reaching a value of $_{gmax}$. A more general form allowing for different rise and decay time-constants is provided by the dual exponential function (Figure B.1):

$$g_{syn}(t) = g_{max}\frac{A}{\tau_2 - \tau_1}(e^{-t/\tau_2} - e^{-t/\tau_1})$$

where A is a normalization constant so that $\max g_{syn}(t) = g_{max}$, and $\tau_1$ and $\tau_2$ ($\tau_2 \geq \tau_1$) are the rise and decay time-constants respectively. If $\tau_1 \to \tau_2$, then the dual exponential function can be identified to an alpha function. The maximum of the function is reached at: $\tau_{max} = \frac{\tau_1\tau_2}{\tau_2-\tau_1}\log\left(\frac{\tau_2}{\tau_1}\right)$.

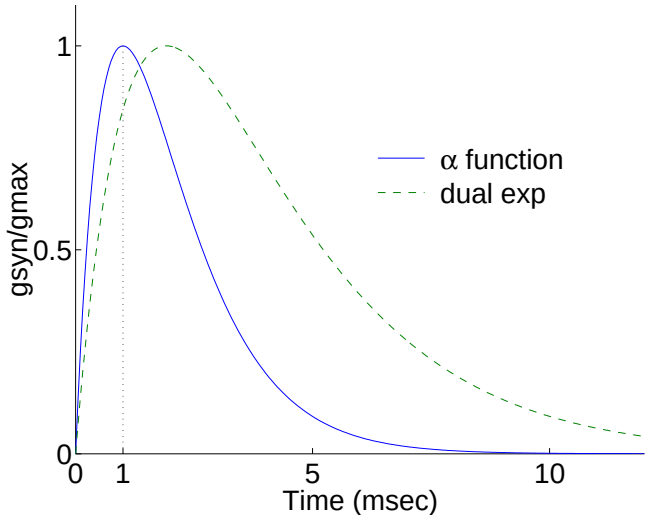


**Figure B.1:** *Alpha and dual exponential functions describing synaptic conductance changes. The time-constants are those used in this work:* $\tau_{syn} = 1ms$, $\tau_1 = 1.5ms$ *and* $\tau_2 = 2.5ms$. *The peak of the dual exponential is reached at* $\tau_{max} = 1.9156$